FINAL PUBLISHABLE REPORT

Grant Agreement number	17IND05
Project short name	MicroProbes
Project full title	Multifunctional ultrafast microprobes for on-the-machine measurements

Project start date and duration:		01 June 2018, 36 + 6 = 42 months
Coordinator: Uwe Brand, PTB Tel: +49 531 592 5111 E-mail: uwe.brand@ptb.de Project website address: https://www.ptb.de/empir2018/microprobes/home/		
Internal Funded Partners: 1. PTB, Germany 2. BAM, Germany 3. CMI, Czech Republic 4. NPL, United Kingdom 5. VTT, Finland	External Funded Partners: 6. bmt, Germany 7. GET, Austria 8. NA, Germany 9. RRI, Finland 10. TT, Germany 11. TUBS, Germany	Unfunded Partners: 12. PT, United Kingdom
RMG:-		

TABLE OF CONTENTS

1 Overview

Traceable micro-measurements of surface form and property are essential in high precision manufacturing industries where the precision control of tools and components and the quality of the finished piece relies on the surface properties achieved. Tool wear and surface contamination are two of the main contributors to a poor surface finish. This project has developed new tactile microprobes for reliable in-line topographical micro-form and roughness measurements that are 20 times faster than conventional methods and methods to measure mechanical surface properties. Users are now able to measure adhesion, stiffness, friction, coating thickness and to detect contaminants through adhesion contrast using contact resonance and force-distance curves.

2 Need

Quality control for manufacturing machines is predominantly carried out off-line, and thus requires the workpiece to be dismounted, measured off-line, and then re-mounted. This is both time consuming and expensive and therefore on-the-machine, in-situ characterisation is urgently needed. Other challenging constraints for the measurement and quality control of machined parts include the size of the small micro-structures to be measured against the strong vibrations of the workpiece, contamination by oil and lubricants and large temperature variations. Fast optical sensors are not adequate for measuring such contaminated surfaces and large measurement artefacts can result leading to measurement deviations up to 100 %.

Another measurement option is the use of tactile small coordinate measuring sensors i.e., microprobes. However, tactile microprobes are currently not small enough or fast enough for use in the quality control of manufacturing machines. Currently, silicon microprobes with 5 mm long cantilevers with integrated silicon tips for roughness measurements in injection nozzles fulfil several requirements like high scanning speed and low probing force, but suffer from strong tip wear, reduced vertical measurement range and a lack of damping. Manufactured parts in industry are also becoming smaller and smaller (micro-metre size), leading to higher requirements concerning the uncertainty of topography and micro-form measurements (where an uncertainty of < 50 nm is required). However, precise measurements are only possible, if the influence of the probing tip shape on the measured profile can be appropriately corrected for.

Further to roughness and topography measurements there is a need in industry to simultaneously measure the mechanical properties of workpieces. Examples of surface layers needing to be measured simultaneously on-the-machine include rubber, polyurethane and wear protection coatings on printing rolls. In addition to the workpiece, a wide variety of tools on micro-finishing machines as well as on roll grinding machines and wear testers also need to be measured on-line.

3 Objectives

The project was focussed on the traceable measurement and characterisation of multifunctional ultrafast microprobes for integration into manufacturing machines. The specific objectives were

1. To develop methods for i) obtaining wear resistant probing tips and to characterize the tips on-the-machine with an uncertainty ≤ 50 nm), ii) the development of the morphological filtering of the tip influence on measurements, iii) setting probing force and scanning speed of microprobes and iv) to develop prototype microprobes with integrated actor, preamplifier and damping for fast measurement of topographic micro-form, structure, roughness and enhanced surface properties like elasticity, adhesion, contamination and thickness of coatings.
2. To develop new large deflection (> 200 µm) and high speed (> 10 mm/s) microprobes for simultaneous measurement of micro-form, roughness, elasticity, adhesion, contamination and thickness of coating layers under industrial conditions. This should include the development of i) pre-deflected cantilevers, ii) actively damped or material-damped cantilevers with thin-film piezoelectric or electro-thermal actuators and iii) thin-film piezoelectric actuator exciting higher-order bending modes suitable for fast CR measurements.
3. To develop validated Contact Resonance (CR) and Force-Distance Curves (FDC) methods for the fast measurement of enhanced surface properties with microprobes on-the machine. The main aim for developing the CR method is the fast detection (< 10 s) of property contrasts on the surface of machined parts on-the-machine, including i) the development of a theoretical model, ii) the determination of the measurement range and resolution, iii) the determination of the lateral resolution,

iv) the measurement of the thickness (10 nm – 1 µm) of soft coatings on hard substrates v) fast measurement of the stiffness and characterisation of the elastic modulus of machined parts on-the-machine and vi) the production of a Good Practice Guide. Aims of the FDC method are i) to detect liquid contamination layers from lubricants through adhesion contrast and extend the range of measurable thicknesses to 10 nm – 500 nm, ii) measurement of the stiffness and of the elastic modulus in the range 100 MPa – 3 GPa, iii) measurement of the thickness (1 - 200 nm) of soft coatings on hard substrates, iv) comparison of FDC results with CR results for a better understanding of the CR method, v) adhesion and friction measurements on the surface of machined parts, vi) to implement the method on-the-machine, vii) to improve the measurement speed and viii) to produce a Good Practice Guide.

4. To develop the integration of microprobes into manufacturing machines, roll grinding machines and wear measuring machines and to develop measuring methods resistant against ambient influences. For the manufacturing machine, this will include i) the development of a new high-speed feed-unit, ii) the development of a probe-machine interface, iii) the development a high-speed data acquisition system and iv) the improvement of resistance against ambient influences. For the roll grinding machines, this will include i) the development of mechatronics to drive the microprobe into contact with the roll, ii) the development of a measurement strategy for roughness measurements, iii) measurements of microprobes with and without damping in comparison to reference probes and iv) the production of a Good Practice Guide. For the wear measuring machines, this will include i) the integration of the microprobes into a pin-on-disc tribometer, ii) the relative wear measurement by an additional reference microprobe, iii) the integration of the microprobes into a reciprocating tribometer and vi) the integration of an additional traverse unit to enable measurement of wear damage during in-situ measurements of wear and v) the production of a Good Practice Guide.
5. To facilitate the take up of the developed technology and measurement infrastructure, in particular the methods for traceable microprobe measurements on-the-machine by the measurement supply chain e.g., manufacturers of machines, standards developing organisations and end-users e.g., high precision mechanical engineering, printing and wear measuring industries. This includes i) direct impact industrial case studies [D8], ii) knowledge transfer, iii) training and iv) uptake and exploitation activities.

4 Results

Objective 1: *To develop methods for obtaining wear resistant probing tips, characterize the tips on-the-machine, development of the morphological filtering, setting probing force and scanning speed of microprobes and to develop prototype microprobes*

Development of microprobes with wear resistant probing tips

Long probe tips are required for measuring structures that are hidden in recessed areas in workpieces. Breitmeier developed new long wear resistant diamond tips of 2 µm radius, 90° conical opening angle and different heights of 0.2 mm, 0.4 mm, 0.6 mm, 0.8 mm, 1 mm and 2 mm [1]. These are available upon request from an industrial supplier and PTB developed a micromanipulator setup to glue the tips to microprobes.

PTB developed a new tip characterizer which for the first time allows to directly image the 2d tip shape of microprobe tips [1]. The method is based on surface profile measurements with the tip to be measured on a new tip characterizer with very sharp edges (s. *Figure 1*) [2]. To avoid damage of the silicon tips to be characterized and of the edges of the silicon tip characterizer during these measurements, a slow scanning speed of 1 µm/s and a small probing force of 15 µN had to be used [3]. A Good Practice Guide was developed describing different methods how to measure tip shape of microprobes. Most of the methods described can also be used on-the-machine.

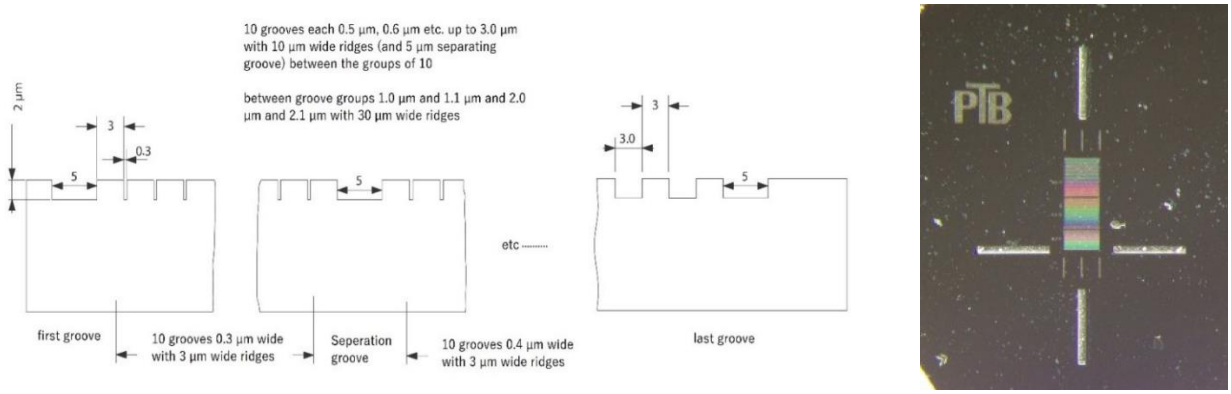

Figure 1 Sketch (left) and photo [4] (right) of the PTB tip characterizer

NPL developed techniques for the evaluation of tip shape using AFM and SEM imaging. The algorithms that were developed for tip reconstruction from the data generated by these instruments were a key aspect of the work. However, although initial work was promising, the techniques were not easy to implement and did not reliably produce usable tip shape information.

FEBID experiments have been carried out by GETec to optimize the mechanical stability of 3D nano-printed tips. Tip wear has been studied using standard self-sensing cantilever structures. The FEBID based tips still show tip wear for high force loads. Therefore, for achieving fast multifunctional measurements on-the-machine diamond tips show the most promising performance.

Based on a paper by Villarubia in which a mathematical morphology-based algorithm was presented for surface imaging and reconstruction, CMI has developed a software tool for performing these operations on profile data. Given a measured profile of the tip, the tool can calculate the image of the actual surface as measured by the tip or reconstruct the actual surface from a measured profile. The source code is available at https://gitlab.com/cmi6014/tip-imaging.

A material point method (MPM) model of a microprobe with tip scanning along the surface has been developed at CMI in order to model tip flight and contact with surface. Unfortunately, the model could not achieve sufficient resolution and performance to be practically usable for real microprobe measurement modelling.

The wear characteristics of silicon tips of microprobes have also been investigated [3] by PTB showing that dependent on the probing force and on the load conditions wear or a successive breaking of the tips occurs. The gentlest scanning method is spiral scanning using a rotary table. For low probing forces of 50 µN and low scanning speed of 0.42 mm/s no wear of the silicon tip was observed after 260 m of measuring length on a steel roughness standard [3]. For ordinary back and forth scanning a partial breakage of the silicon tips was observed [3] leading to blunt tips with approximately 3 µm radius. For many industrial surface texture measurements this radius is quite sufficient. For applications where smaller radii or exactly 2 µm radius is required, the developed diamond tips can be used.

An important measurement error of tactile probes is the occurrence of tip-flight at high measurement speeds. This has been studied through developing a theoretical dynamic model, measuring their resonant response, and performing tip-flight experiments on surfaces with sharp variations. Two microprobes were investigated and compared: one with the ordinary integrated silicon tip and one with a diamond tip glued to the end of the cantilever. The result indicates that the microprobe with the silicon tip has high trackability for measurements up to traverse speeds of 10 mm/s, while the resonant response of the microprobe with diamond tip needs to be improved for the application in high-speed topography measurements [5].

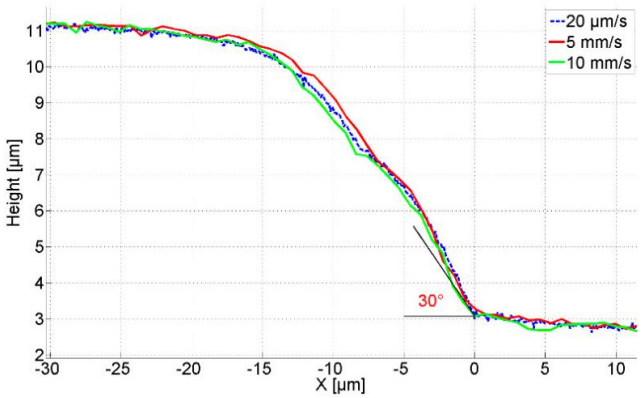

Figure 2 Measured profiles with the CAN50-2-5 microprobe with integrated silicon tip. (a) Measured profiles on artifact A (30° inclined sidewall) with an initial static probing force of 96 µN, at different traverse speeds (s. Fig. 8a in [5])

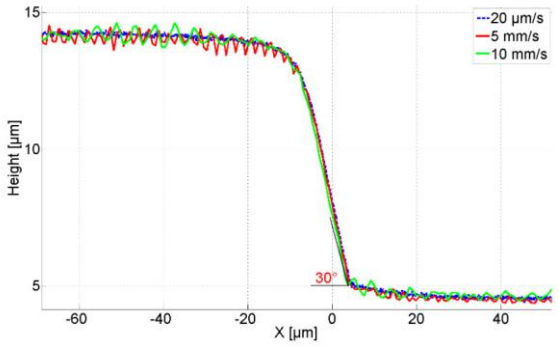

Figure 3 Measured profiles on artifact A using the microprobe with diamond tip with an initial static probing force of 96 µN, at different traverse speeds (s. Fig. 9 in [5])

Setting maximum probing force and maximum scanning speed of microprobes

During fast tactile topography measurements, the inertia of the microprobe cantilever creates dynamic forces which might lead to tip flight and thus measurement errors. To prevent from tip flight, usually the highest possible probing forces are used. These are mainly given by the hardness of the surface to be measured. A Good Practice Guide was developed which helps end-users of microprobes to set the probing force and the maximum scanning speed of their microprobing system for reliable topography and roughness measurements.

The maximum scanning speed of conventional stylus instruments is limited by the inertia of the probe system. For typical probe masses of 1 g the maximum scanning speed of such probing systems is limited to approximately 0.5 mm/s [6]. For smaller stylus masses of 5 mg scanning speeds of 2.5 mm/s were obtained supported by an analytical model describing a simple pivoting stylus [6]. This model was used here to simulate the dynamical properties of 5 mm long cantilever type piezoresistive microprobes. A further measurement deviation might occur due to scratching of surfaces during measurement. To model this, an approach of Flores describing the elasto-plastic scratching of surfaces for spherical indenters [7] was used. The Good Practice Guide developed assumes an optimum damping of the microprobes in such a way that no eigenfrequencies are excited.

Maximum probing force

For standard two-dimensional roughness profile measurements, a maximum probing force of 750 µN is recommended for tip radii down to 2 µm. This recommendation is only valid for hard surfaces comparable to steel. For softer materials the probing force needs to be lower to prevent the scratching of these surfaces. To describe the plastic scratch depth d_{pl} a formula given by Flores [7] for metals was used. It describes the scratch depth to be proportional to probing force F and inversely proportional to the yield strength Y and the tip radius r. For materials with vanishing strain hardening coefficient it was assumed that the hardness H is approximately three time the yield strength Y [8]. A threshold for tolerable scratching depth of surfaces of less than 10^{-3} of the tip radius was assumed to estimate the maximum probing force F_{max} for different hard metals and different tip radii:

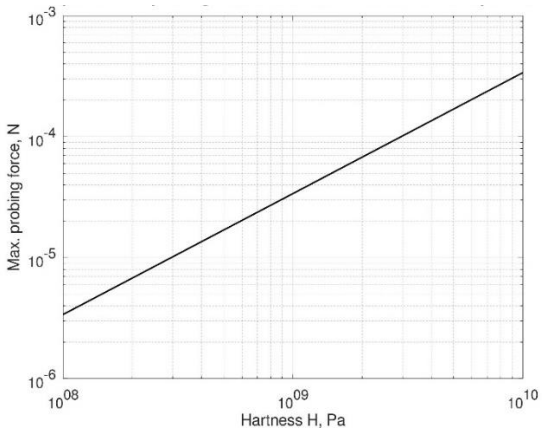

Figure 4 Maximum probing force versus hardness of the material to be measured for a 2 µm tip radius

$$F_{max} < \frac{2.7 \cdot \pi \cdot r^2 \cdot H}{1000}$$

Maximum permissible probing forces range from 9 µN on soft metals like gold and brass to 289 µN on hard metals like chromium for a 2 µm tip radius.

Maximum scanning speed

To describe tip flight the model of Morrison [6] was used, who modelled the maximum scanning speed of a stylus instrument with pivoting stylus. Sinusoidal surface profiles with surface wavelength λ and amplitude A_1 were assumed. The inertial mass m_i of the microprobe mainly consists of the mass of the cantilever with length L, width w, thickness d and density ρ. For microprobes with diamond tip the mass of the tip has to be added to the inertial mass m_i. For microprobes with silicon tip the mass of these tips can be neglected. Dynamic forces created at steep slopes of the profile lead to tip flight. Thus, not the static cantilever mass has to be considered, but the effective mass of the cantilever m_{eff} [9] which is $m_{eff} = \frac{33}{140} m_i$. For standard CAN50-2-5 microprobes from CiS [10,11] with 5 mm length, 200 µm width and a thickness of 50 µm an effective mass m_{eff} of 0.027 mg results. For sinusoidal surface structures it is assumed that the minimum surface wavelength λ_{min} that can be measured is larger than four times the tip radius ($\lambda_{min} > 4 \cdot r$). Thus, for a tip radius r = 2 µm the smallest measurable surface wavelength is λ_{min} = 8 µm. Assuming further a surface amplitude A_1 of 0.1 µm then the maximum scanning speed v_{max} can be calculated (s. *Figure 6*).

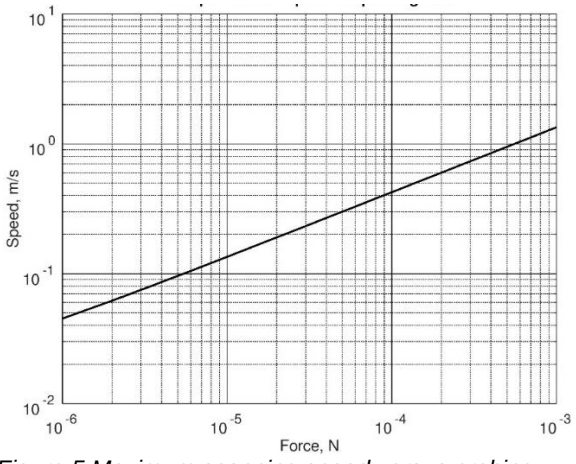

Figure 5 Maximum scanning speed versus probing force for 5 mm long piezoresistive microprobes with 2 µm tip radius on sinusoidal surface structures with 0.1 µm amplitude and 8 µm surface wavelength

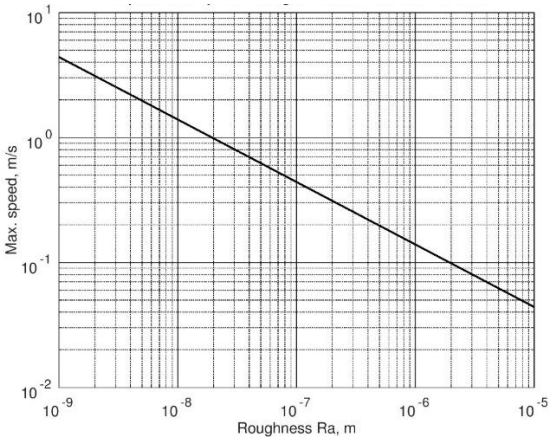

Figure 6 Maximum scanning speed of a microprobe with 2 µm tip radius on a nickel surface (hardness H_{Ind} = 5 GPa) versus roughness of the nickel surface

Thus, for sinusoidal surface profiles down to 8 µm surface wavelength and up to 100 nm amplitude probing forces in the range from 10 µN to 300 µN lead to maximum scanning speeds of the microprobe with 2 µm tip radius from 70 mm/s to 350 mm/s. For larger sinusoidal amplitudes A_1 the scanning speed reduces inversely proportional to the square root of A_1. Often the surface roughness but not the surface amplitude is known. The arithmetic mean roughness R_a of a sinusoidal surface structure with wavelength λ is proportional to the amplitude A_1: $R_a = \frac{2A_1}{\pi}$. Thus, the maximum scanning speed v_{max} is: $v_{max}(F) = \sqrt{\frac{3 \cdot \lambda^2 \cdot (2F + m_{eff} \cdot g)}{4 \cdot \pi^3 \cdot R_a \cdot m_{eff}}}$. As an example, the maximum scanning speed of a microprobe with 2 µm tip radius on a nickel surface varies from 4 m/s for mirror like smooth surfaces (R_a = 1 nm) to 40 mm/s for very rough surfaces (R_a = 10 µm) (s. *Figure 6*).

Prototype microprobes with integrated actor, preamplifier and damping for fast measurement of topographic micro-form, structure, roughness and enhanced surface properties like elasticity, adhesion, contamination and thickness of coatings

Different microprobe holders were developed and are available for the integration of microprobes into different machines:

a. multipurpose micro-probe holder with front-end electronics designed for topography and CR, layout available [12]

b. microprobe with electrothermal [13] and piezoelectric actuator designed for high-order CR, layouts and MEMS process parameters (tested only with electrothermal actuator [14]) available

c. adapter for roll-grinding machines with overload protection [15]

d. adapter for wear measuring machines with overload protection [16]

e. micro-probe holder with front-end electronics and adapter for Cypher AFM (Asylum Research, Oxford Instruments, Santa Barbara, USA) [17] designed for topography, CR, FDC and lateral force sensing, layout available

f. adapters for commercially available high-speed AFMs (s. *Figure 7* and *Figure 8*)

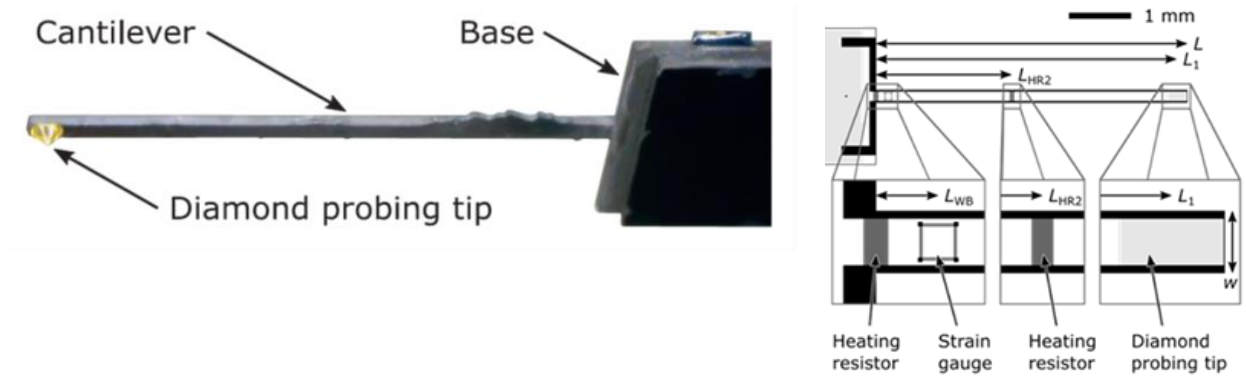

Figure 7 Electrothermal-actuated 5 mm long microprobe with glued wear resistant diamond tip (left). Two heating resistors (right) are positioned at the cantilever topside for efficient higher-mode actuation at uniform signal amplitudes in CR with materials of different elasticity. These resistors are fabricated simultaneously with the piezoresistive Wheatstone bridge, i. e., the corresponding lithography mask had to be modified but no additional process step is necessary.

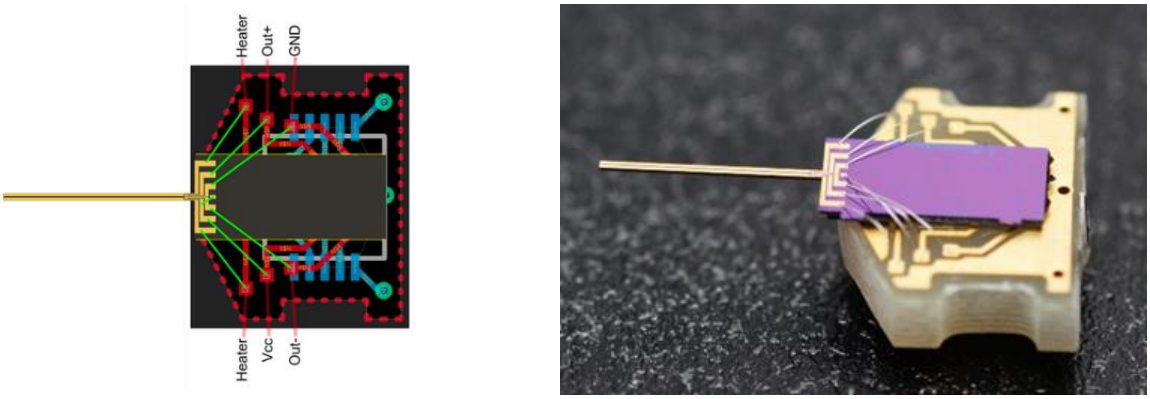

Figure 8 5 mm long microprobe with electrothermal actuators mounted and bonded on holder PCBs from GETec for operation in their AFSEM®

Conclusion

To summarize, the project successfully achieved the objective by

- the development of new wear resistant diamond tips by partner Breitmeier
- the development of a new method by PTB to characterize the probing tips on-the-machine by using a new silicon tip characterizer

- the development of a software tool for morphological filtering of measured profiles to subtract the influence of the tip from the profile by partner CMI
- the development of a Good Practice Guide for setting maximum probing force and scanning speed of microprobes in order not to scratch the surfaces to be measured and so that no tip-flight is obtained by PTB
- the development of prototype microprobes by partners TU Braunschweig, BAM, VTT, RRI, NPL, GETec and nano analytik

[1.] Brand, U.; Xu, M.; Doering, L.; Langfahl-Klabes, J.; Behle, H.; Bütefisch, S.; Ahbe, T.; Peiner, E.; Völlmeke, S.; Frank, T.; et al. Long Slender Piezo-Resistive Silicon Microprobes for Fast Measurements of Roughness and Mechanical Properties inside Micro-Holes with Diameters below 100 µm. *Sensors* **2019**, *19*, 1410, doi:10.3390/s19061410.

[2.] Brand, U. Good Practice Guide "Calibration of Tip Radius of Fast Microprobes on-the-Machine" Available online: https://www.ptb.de/empir2018/fileadmin/documents/empir/MicroProbes/Good_Practice_Guide_No_1_MicroProbes_Calibration_of_tip_radius_of_fast_microprobes_on_the_machine.pdf.

[3.] Xu, M.; Zhou, Z.; Ahbe, T.; Peiner, E.; Brand, U. Investigating the Microprobe Silicon Tip Geometry Variation in the Roughness Measurement with a Tip Characterizer. *Sumitted Sens.* **2022**.

[4.] Brand, U.; Gao, S.; Doering, L.; Li, Z.; Xu, M.; Buetefisch, S.; Peiner, E.; Fruehauf, J.; Hiller, K. Smart Sensors and Calibration Standards for High Precision Metrology.; 2015; Vol. Proc. SPIE 9517, pp. 95170V-95170V – 10.

[5.] Xu, M.; Li, Z.; Fahrbach, M.; Peiner, E.; Brand, U. Investigating the Trackability of Silicon Microprobes in High-Speed Surface Measurements. *Sensors* **2021**, *21*, 1557, doi:10.3390/s21051557.

[6.] Morrison, E. The Development of a Prototype High-Speed Stylus Profilometer and Its Application to Rapid 3D Surface Measurement. *Nanotechnology* **1996**, *7*, 37.

[7.] Flores, S.E.; Pontin, M.G.; Zok, F.W. Scratching of Elastic/Plastic Materials With Hard Spherical Indenters. *J. Appl. Mech.* **2008**, *75*, 061021–061021, doi:10.1115/1.2966268.

[8.] Cahoon, J.R.; Broughton, W.H.; Kutzak, A.R. The Determination of Yield Strength from Hardness Measurements. *Metall. Trans.* **1971**, *2*, 1979–1983, doi:10.1007/BF02913433.

[9.] Skrzypacz, P.; Nurakhmetov, D.; Wei, D. Generalized Stiffness and Effective Mass Coefficients for Power-Law Euler–Bernoulli Beams. *Acta Mech. Sin.* **2020**, *36*, 160–175, doi:10.1007/s10409-019-00912-8.

[10.] Frank, T.; Doering, L.; Heinrich, G.; Thronicke, N.; Löbner, C.; Steinke, A.; Reich, S.; others Silicon Cantilevers with Piezo-Resistive Measuring Bridge for Tactile Line Measurement. *Microsyst. Technol.* **2014**, *20*, 927–931.

[11.] CiS Forschungsinstitut Für Mikrosensorik GmbH, Piezoresistive Microprobes CAN50-2-5.

[12.] Fahrbach, M.; Friedrich, S.; Cappella, B.; Peiner, E. Calibrating a High-Speed Contact-Resonance Profilometer. *J. Sens. Sens. Syst.* **2020**, *9*, 179–187, doi:https://doi.org/10.5194/jsss-9-179-2020.

[13.] Setiono, A.; Fahrbach, M.; Deutschinger, A.; Fantner, E.J.; Schwalb, C.H.; Syamsu, I.; Wasisto, H.S.; Peiner, E. Performance of an Electrothermal MEMS Cantilever Resonator with Fano-Resonance Annoyance under Cigarette Smoke Exposure. *Sensors* **2021**, *21*, 4088, doi:10.3390/s21124088.

[14.] Fahrbach, M.; Peiner, E.; Xu, M.; Brand, U. A5.4 Self-Excited Contact Resonance Operation of a Tactile Piezoresistive Cantilever Microprobe with Diamond Tip. *SMSI 2021 - Sens. Instrum.* **2021**, 73–74, doi:10.5162/SMSI2021/A5.4.

[15.] Teir, L.; Lindstedt, T.; Widmaier, T.; Hemming, B.; Brand, U.; Fahrbach, M.; Peiner, E.; Lassila, A. In-Line Measurement of the Surface Texture of Rolls Using Long Slender Piezoresistive Microprobes. *Sensors* **2021**, *21*, 5955, doi:10.3390/s21175955.

[16.] Gee, M. Good Practice Guide "In-Situ Wear Damage Measurement Using Fast Microprobes with Integrated Feed-Unit" Available online: https://www.ptb.de/empir2018/fileadmin/documents/empir/MicroProbes/Good_Practice_Guide_No_6_In-situ_wear_damage_measurement_using_fast_microprobes_with_integrated_feed-unit.pdf.

[17.] Fahrbach, M.; Friedrich, S.; Behle, H.; Xu, M.; Cappella, B.; Brand, U.; Peiner, E. Customized Piezoresistive Microprobes for Combined Imaging of Topography and Mechanical Properties. *Meas. Sens.* **2021**, *15*, 100042, doi:10.1016/j.measen.2021.100042.

Objective 2: *To develop new large deflection (> 200 µm) and high speed (> 10 mm/s) microprobes for simultaneous measurement of micro-form, roughness, elasticity, adhesion, contamination and thickness of coating layers under industrial conditions.*

Pre-deflected microprobes

Due to a lack of CAN50-2-5 microprobes at the beginning of the project we performed bending experiments with available dummy cantilevers (CAN15-3-2, l = 3 mm, w = 100 µm, h = 25 µm). We used a pulsed Nd:YAG laser operated at 520 nm wavelength, 500 mW of power, 6 m/s scanning velocity and 200 kHz pulse frequency and achieved a predeflection corresponding to the required ≈ 200 µm for the CAN50-2-5. In this process, however, formation of 10-15 µm deep notches was observed across the cantilever width and local oxidation of silicon, which indicated the risk of early failure due to a generated local stress. Therefore, laser bending was not further considered for ensuring large-deflection operation of the CAN50-2-5.

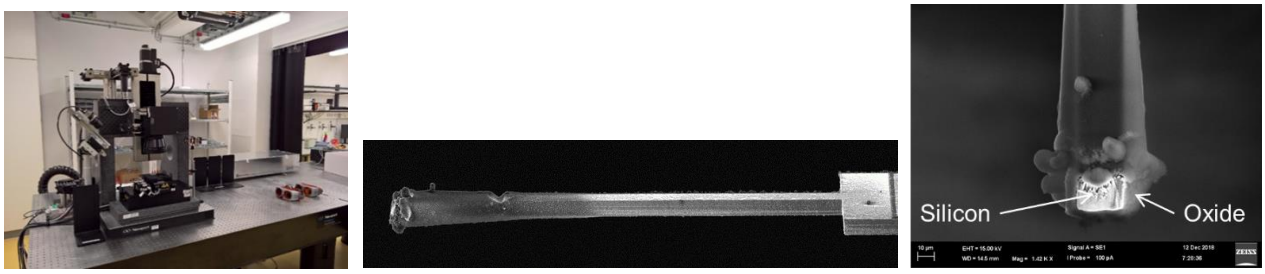

Figure 9 Setup and results of laser bending of silicon cantilevers.

We then investigated weight-/strain-induced pre-deflection using a photoresist (AZ5214E) layer dipping-deposited on a CAN50-2-5 cantilever, which resulted in a pre-deflection of 75 µm. Gluing of a 1000-µm-high diamond tip to the microprobe, however, could add only less than 1 µm of further deflection.

Figure 10 CAN50-2-5 bent-down by 75 µm using a dip-deposited photoresist (AZ5214E) layer.

Finally, even without pre-deflection, 120 µm and 500 µm of total deflection were measured at NL ≈ 0.4 % and NL ≈ 1.0 %, respectively, with CAN50-2-5 microprobes using the PTB and TUBS setups for load-deflection measurements. We conclude that pre-deflection will be of minor significance for ensuring the required measurement range of ± 200 µm with CAN50-2-5 microprobes.

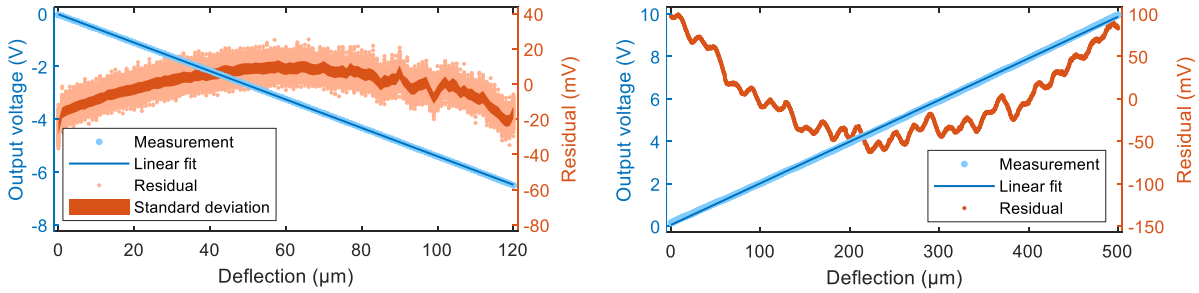

Figure 11 Load-deflection curves with CAN50-2-5 microprobes yielding nonlinearities of NL ≈ 0.4 % (left) and NL ≈ 1.0 % (right).

Actively damped or material-damped cantilevers with thin-film piezoelectric or electro-thermal actuators

Due to problems and delays during fabrication of thin-film piezoelectric actuators we concentrated first on chip-size piezoelectric and electro-thermal actuators. For active damping a circuit for quality-factor (Q) control was employed by GET based on delay, amplification and mixing of the input signal from the microprobe with a working frequency set in a Lock-In amplifier. It was tested in their AFSEM® in high-speed measurements with free-standing graphene membranes, provisionally with thermal-actuated AFM cantilevers. Furthermore, GET with support of TUBS developed a CAN50-2-5 microprobe holder for their AFSEM® which could be operated in free oscillation modes but so far not in CR.

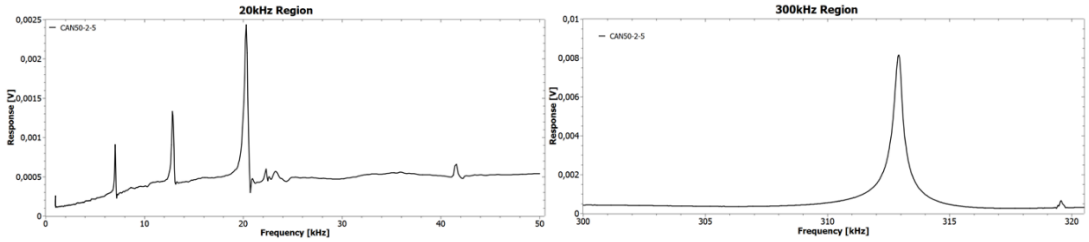

Figure 12 Frequency sweep of CAN50-2-5 microprobe measured in a AFSEM®.

Passive damping of a CAN50-2-5 using dipping-deposited photoresist (AZ5214E) yielded for the 1st mode and the 2nd mode amplitudes reduced by and 2 dB and 20 dB, respectively. For better reproducibility we then used mixtures of epoxy glue, isopropyl alcohol and glycerol, manually deposited using a plastic fiber according to a recipe by GET, which, however was affected by formation of bubbles. This problem was overcome using a PC-controlled picoliter-droplet dispenser for depositing the final mixture of epoxy : isopropanol : glycerol of 2 : 10 : 1 reproducibly at 10 equidistant points along the CAN50-2-5 cantilever axis showing only few bubbles. Before wire bonding, droplets on contact pads had to be removed after the final coating had cured.

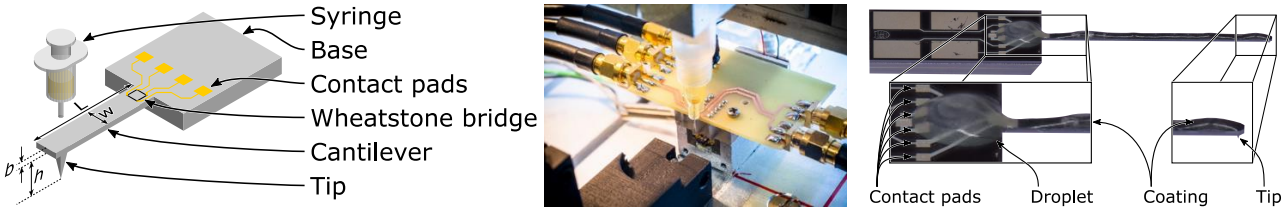

Figure 13 PC-controlled picoliter-droplet dispenser with a tip inner diameter of 0.1 mm.

A 2-times-deposited cantilever (0.15 bar for 10 ms per droplet) showed a 16 dB amplitude damping of the 1st free mode. A similar damping was observed by PTB in CR spectra induced by scanning the CAN50-2-5 microprobe at 10 mm/s on sandpaper. Subsequently, up to 10 deposition sequences were then done showing an exponential increase of total damping-layer thickness with the number of depositions. Analysis of the resulting 1st free mode according to Eq. (2.1), which took parasitic excitation-detection cross-talk into account [2.4, 2.5], yielded an exponential decrease of its quality factor with the number of coatings.

$$U = \frac{(U_{\mathrm{res}}/Q)\exp(i\varphi_{\mathrm{del}})}{(i\omega/\omega_{\mathrm{res}})^2 + i\omega/(Q\omega_{\mathrm{res}}) + 1} + U_{par}exp\left(i\varphi_{par}\right) \qquad (2.1)$$

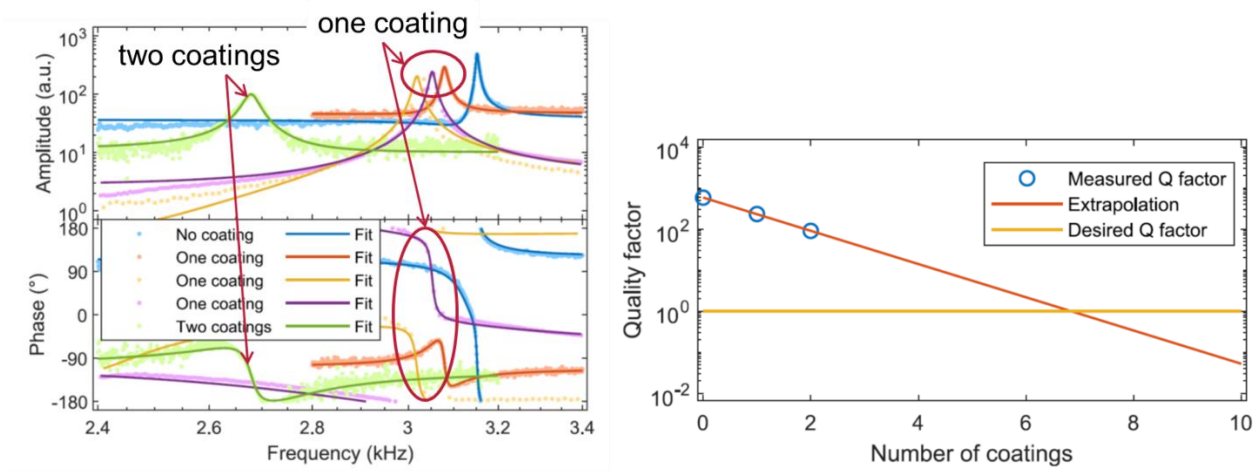

Figure 14 Frequency sweep across 1st free oscillation mode of several-times deposited CAN50-2-5 microprobe.

Extrapolation towards the target value of Q = 1 yielded 7 depositions, after which critical damping should be attained [2.3].

Furthermore, a new microprobe with integrated electrothermal actuators was designed according to dimensions of the CAN50-2-5 microprobe, except its thickness, which was increased to ≈ 100 µm for larger stiffness. For fabrication, a new process based on bulk silicon micromachining was developed and executed

in the clean-room lab of TUBS. Fabricated samples of the new microprobe were characterized and compared with finite-element modelling (FEM) using COMSOL Multiphysics. Electrothermal actuation was optimized for second-higher-mode CR operation and uniform signal amplitudes when probing materials of different elasticity. Finally, a diamond probing tips was glued by PTB. With these microprobes a deflection amplitude of $\Delta z \approx \pm 15$ µm was achieved in resonance with $Q \approx 1000$, which corresponds to $\Delta z \approx \pm 15$ nm at low frequencies. Below 0.1 Hz we could achieve deflections even up to $\Delta z \approx 2$ µm.

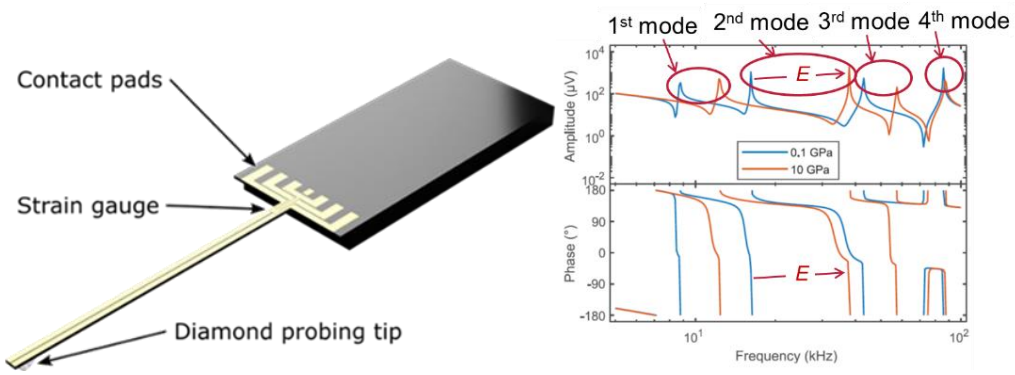

Figure 15 New microprobe with integrated electrothermal actuator for CR.

Measurements with bulk Al and a thin polymer layer on Si were analyzed using Fano-resonance fits [2.4, 2.5]. Both showed an increase of contact stiffness k^* with probing force and a corresponding frequency shift as well as line broadening of the 1st mode CR, which can be expected for viscoelastic materials [2.6].

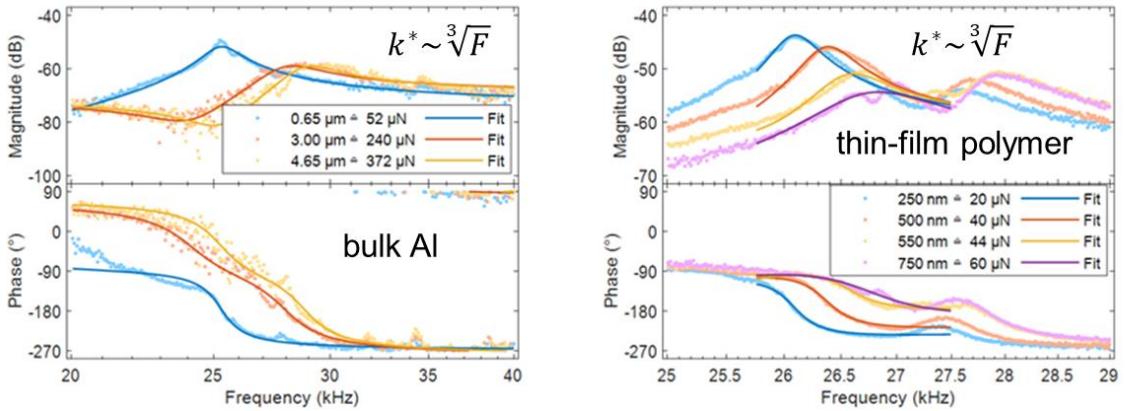

Figure 16 CR measurements with bulk Al and a thin-film polymer using a new microprobe with integrated electrothermal actuator and diamond tip.

Thin-film piezoelectric actuator exciting higher-order bending modes suitable for fast CR measurements

Due to problems and delays during fabrication of thin-film piezoelectric actuators we concentrated first on chip-size piezoelectric actuators (PI, PL055.30) glued below the microprobe for base-point excitation and performed our CR measurements with a holder PCB, which was developed for the CAN50-2-5 microprobe. For this, a software-phase-locked loop (SPLL) based measurement system with automatic gain control (AGC) was developed. It can be operated at a sample rate of 300 S/s in the frequency range from 1 kHz to 500 kHz [2.7].

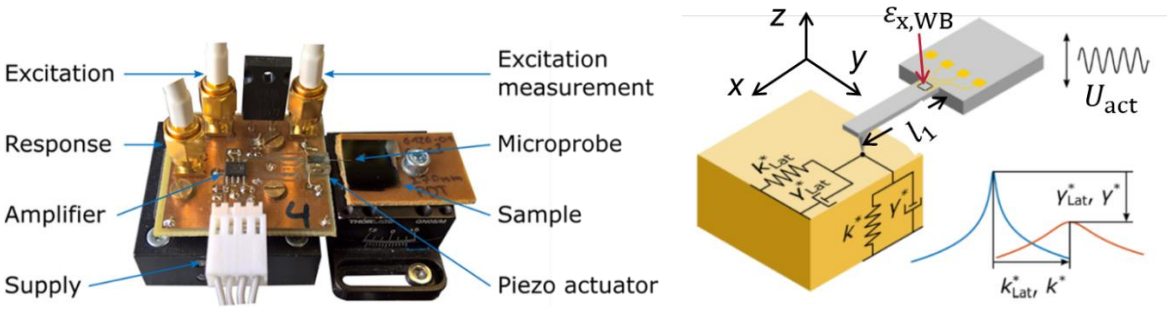

Figure 17 CAN50-2-5 microprobe with a chip-size piezoactuator (PI, PL055.30) for base-point excitation.

We then prepared layers of 5 different polymer materials (photo-, e-beam- and nano-imprint resist, as well as the conducting polymer PEDOT) on Si for CR measurements [2.8, 2.9] and found dependences of 1st and 2nd mode CR on layer thickness in the range of few nm to few µm and on force in the tens to hundreds of µN range. Based on this we developed a procedure for quantitative evaluation of contact stiffness and deformation during CR measurement, which is based on a thorough calibration procedure. With it a square-root dependence of contact stiffness of the 1st, 2nd and 3rd CR mode on deformation was found with a thin polymer film on silicon delivered by BAM, which can be expected according to the Hertz mechanical contact theory (Eq. 2.2):

$$k^* = \frac{3}{2} E_{\mathrm{red}} \sqrt{R} \sqrt{D} \tag{2.2}$$

Plastic deformation or substrate effect at large deformations of several hundreds of µm were discussed as possible reasons for the measured mismatch of the 3 curves. A value of the Young's modulus of the polymer film was not determined due to the missing knowledge on (Si) tip diameter.

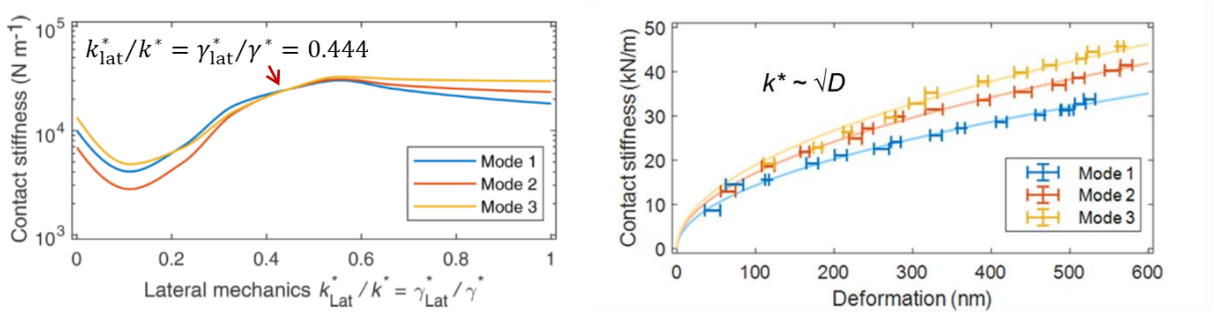

Figure 18 Lateral-to-vertical viscoelasticity and contact stiffness of 1st, 2nd and 3rd CR modes on PnBMA [2.10].

A microprobe with integrated piezoelectric actuator was designed and modelled using FEM showing high sensitivity of the 1st mode to the elasticity of different probed materials in the range around 1 GPa.

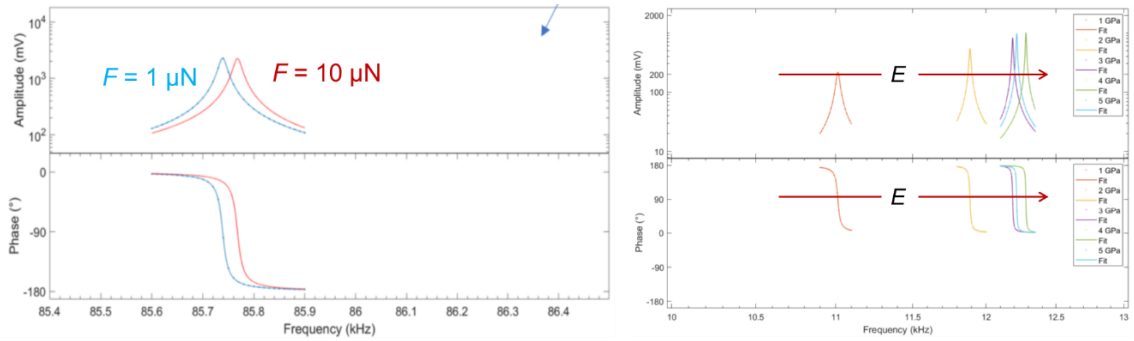

Figure 19 FEM of microprobe with thin-film piezoelectric actuator in contact, 4th CR mode under varying load (left) and 1st CR at different Young's moduli (right).

AlN was selected as thin-film piezoelectric actuator material for the microprobes. For sputter deposition of AlN a process was developed on a P395 – 4″ HV sputter deposition system from Bestec, Berlin. To avoid short cuts via pinholes in the AlN, they were filled by thermal oxidation of the silicon substrate. A selective AlN

patterning process was investigated starting with 5 different wet etching solutions. Best results were found with 85% phosphoric acid and the TechniEtch Al80 solution from Microchemicals GmbH, Ulm, Germany. Finally, piezoelectric function of our thin-film AlN could be demonstrated. Microprobe fabrication could not be completed within the project term.

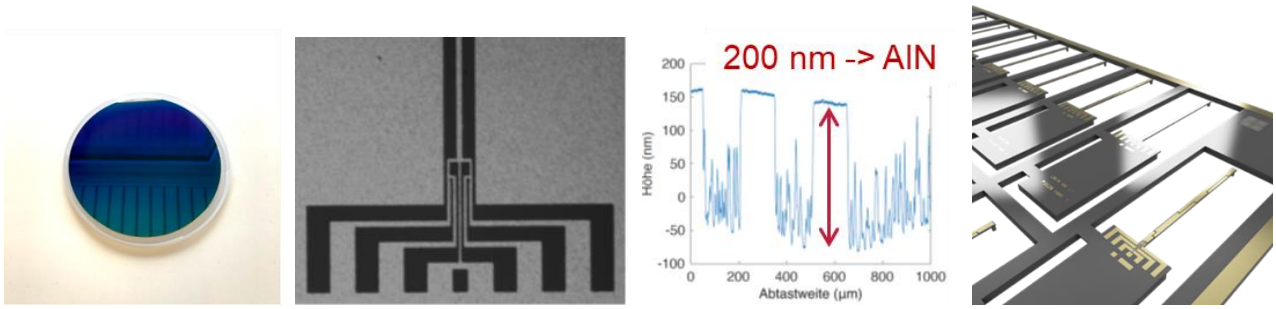

Figure 20 Thin-film AlN on silicon, patterned using TechniEtch Al80 at 20 to 120°C, 23 min and microprobe design.

Conclusion

To summarize, partner TUBS assisted by the partners BAM, GET, NA and PTB successfully achieved the objective by

- successfully using laser bending for predeflecting CAN50-2-5 microprobes corresponding to the required large deflection of ≈ 200 µm
- developing and verifying a new method during scanning at 10 mm/s on sandpaper using material damping of CAN50-2-5 microprobes based on picoliter-droplet dispensing of an epoxy-isopropanol-glycerol mixture
- developing and verifying new processes for fabricating cantilever microprobes with thin-film piezoelectric and electro-thermal actuators
- developing a novel setup based on CAN50-2-5 and electro-thermal-actuated microprobes, which was developed and tested in contact resonance (CR, up to the 4th higher mode) measurements of elasticity and thickness of thin polymer coating layers.

[2.1] Michael Fahrbach, Erwin Peiner, “Entwicklung eines taktilen Mikrotaster-Messsystems für Hochgeschwindigkeitsmessung von Form, Rauheit und mechanischen Eigenschaften”, *20. ITG/GMA-Fachtagung „Sensoren und Messsysteme 2019”*, 25.-26. Juni 2019, Kongresszentrum Nürnberg, (AMA Service GmbH, Wunstorf, 2019), pp. 720-725; DOI: 10.5162/sensoren2019/P2.10; https://www.ama-science.org/proceedings/details/3479.

[2.2] Michael Fahrbach, Sebastian Backes, Heinrich Behle, Min, Xu, Brunero Cappella, Uwe Brand, Erwin Peiner, “Customized piezoresistive microprobes for combined imaging of topography and mechanical properties”, *Measurement: Sensors* **15** (2021) 100042 (10pp); https://doi.org/10.1016/j.measen.2021.100042

[2.3] Michael Fahrbach, Wilson Ombati Nyang’au, Oleg Domanov, Christian H. Schwalb, Min Xu, Zhi Li, Christian Kuhlmann, Uwe Brand und Erwin Peiner, “Gedämpfte Silizium Mikrotaster für Hochgeschwindigkeits-Rauheitsmessungen, Damped silicon micro probes for high-speed roughness measurements”, *Proc. MikroSystemTechnik Kongress 2021*, 8.-10. November 2021, Stuttgart, (VDE-Verlag, Berlin 2021).

[2.4] Andi Setiono, Maik Bertke, Wilson Ombati Nyang’au, Jiushuai Xu, Michael Fahrbach, Ina Kirsch, Erik Uhde, Alexander Deutschinger, Ernest J. Fantner, Christian H. Schwalb, Hutomo Suryo Wasisto, Erwin Peiner, “In-plane and out-of-plane MEMS piezoresistive cantilever sensors for nanoparticle mass detection”, *Sensors* **20** (2020) 618 (18pp); https://doi.org/10.3390/s20030618.

[2.5] Andi Setiono, Michael Fahrbach, Alexander Deutschinger, Ernest J. Fantner, Christian H. Schwalb, Iqbal Syamsu, Hutomo Suryo Wasisto, Erwin Peiner, “Performance of an Electrothermal MEMS Cantilever Resonator with Fano-Resonance Annoyance under Cigarette Smoke Exposure”, *Sensors* **21** (2021) 4088 (19pp); doi: 10.3390/s21124088, https://www.mdpi.com/1424-8220/21/12/4088.

[2.6] Michael Fahrbach, Min Xu, Uwe Brand and Erwin Peiner, “Self-excited Contact Resonance Operation of a Tactile Piezoresistive Cantilever Microprobe with Diamond Tip”, *SMSI 2021 Conference – Sensor and Measurement Science International*, pp. 73 – 74; DOI 10.5162/SMSI2021/A5.4; https://www.ama-science.org/proceedings/details/3948.

[2.7] Michael Fahrbach, Linus Krieg, Tobias Voss, Maik Bertke, Jiushuai Xu and Erwin Peiner, “Optimizing a cantilever measurement system towards high speed, nonreactive contact-resonance-profilometry”, *32th European Conf. Solid-State Transducers (Eurosensors 2018)*, Granz, Österreich, Sept., 9-12; *Proceedings* **2** (2018) 889 (5pp); doi:10.3390/proceedings2130889, https://www.mdpi.com/2504-3900/2/13/889

[2.8] Michael Fahrbach, Sebastian Backes, Brunero Cappella, Erwin Peiner, “Scanning characterization of polymer coating layers using contact resonance with piezoresistive microprobes”, *euspen’s 19th International Conference & Exhibition*, Bilbao, ES, 3 - 7 June 2019, submission ICE19274, https://www.euspen.eu/knowledge-base/ICE19274.pdf

[2.9] Michael Fahrbach, Erwin Peiner, “Higher-Mode Contact Resonance Operation of a High-Aspect-Ratio Piezoresistive Cantilever Microprobe”, *Proc. SMSI 2020 Conference – Sensor and Measurement Science International*, pp. 89 – 90; DOI: 10.5162/SMSI2020/A6.3, https://www.ama-science.org/proceedings/details/3656.

[2.10] Michael Fahrbach, Sebastian Friedrich, Brunero Cappella, Erwin Peiner, “Calibrating a high-speed contact-resonance profilometer”, *J. Sens. Sens. Syst.* **9** (2020) 179–187, https://doi.org/10.5194/jsss-9-179-2020.

Objective 3: *To develop validated Contact Resonance (CR) and Force-Distance Curves (FDC) methods for the fast measurement of enhanced surface properties with microprobes on-the machine*

Contact resonance (CR) methods

A CR method with microprobes integrated in a Cypher AFM (Asylum Research – Oxford Instruments, Santa Barbara, USA) has been developed. The excitation is actuated through the sample, which is glued to a contact-resonance sample holder by means of a two-component epoxy. Two kinds of measurements have been performed.

In single-point CR measurements, a frequency sweep (tune)is performed while the tip is in contact with the sample and contact-resonance is determined. To avoid sample damage, every point measurement is done on a different spot on the sample. Each value is averaged over four to six separate measurements. In different series of measurements, the static force exerted on the sample by the tip has been varied. A sufficiently small excitation amplitude has been chosen for the frequency sweep, so that the tip always remains in contact.

In dual AC resonance tracking (DART) mode, the cantilever is excited at two frequencies on either side of the resonance frequency f_n, which permits to track f_n while scanning the sample in contact.

It has been shown that CR modes such as DART, performed with the tip in permanent contact with the sample, are likely to wear compliant polymer samples and to modify the sample surface, notably the roughness, and as a consequence the contact area with the tip. Scanning CR methods are therefore not suitable for quantitative measurements of the elastic modulus on polymers [3.1]. Nevertheless, it was possible to perform DART measurements exploiting the piezoresistive signal at the edge of an AZ 5214E photoresist film on silicon [2]. Main results are shown in Figure 21. The contrast in the frequency map between the bare silicon and the polymer-coated areas is not very pronounced. This is due to the small differences in modulus between substrate and a thin film, but also to the large tip radius. Nevertheless, in the histogram of the contact resonance frequency, the two materials can be distinguished. The histogram was fitted with the sum of two Gauss curves, centered at 14.145 kHz with a width of 35 Hz (polymer film) and 14.200 kHz with a width of 34 Hz (silicon). The fluctuations of the contact resonance frequency visible in the map originate probably from contamination of the tip with polymer particles.

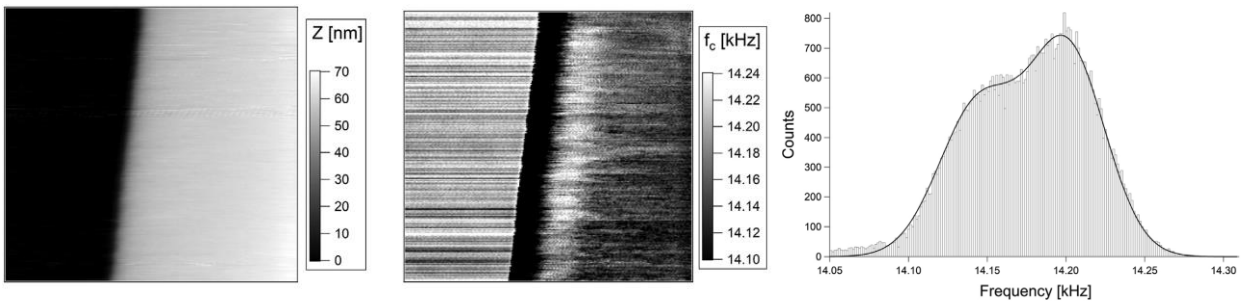

Figure 21 DART-measurement at the border of an AZ 5214E film on silicon, acquired by exploiting the piezoresistive signal. Topography (left) and contact resonance frequency (middle). The area of the maps is 30 µm × 28:115 µm. The bare silicon is on the left side of the maps, the polymer film on the right side. (Right) Histogram of the contact resonance frequency fitted with a double Gauss curve. Adapted from Ref [3.2].

Point measurements have been shown to enable the accurate determination of the elastic modulus of glass, PS, and PMMA. Previous to measurements [3.1], the common equation describing the dynamic response of the cantilever as a function of the contact stiffness has been approximated in the form

$$f_n = \left(\frac{x_n L}{x_n^0 L}\right)^2 f_n^0 = \left[\frac{5}{4}\pi \frac{1}{\gamma x_n^0 L}\left(1 - \left(\frac{5}{12}\pi\right)^2 \frac{k_c}{\sqrt[3]{RE_{tot}^2 F}}\right)\right]^2 f_n^0. \quad (3.1)$$

with f_n and f_n^0 the contact resonance frequency and the free resonance frequency for the n^{th} flexural mode, $x_n L$ and $x_n^0 L$ the wavenumbers for the contact and free flexural mode n, γ a parameter, k_c the elastic constant of the cantilever, R the tip radius, E_{tot} the reduced elastic modulus and F the static force.

The exact equation permits only to calculate the force as a function of the frequency; on the contrary, the approximation allows also to express the frequency as a function of the force, thus enabling to fit curves of the frequencies acquired with different static forces and finally to determine the elastic modulus of the sample.

The main results of the measurements are shown in Figure 22.

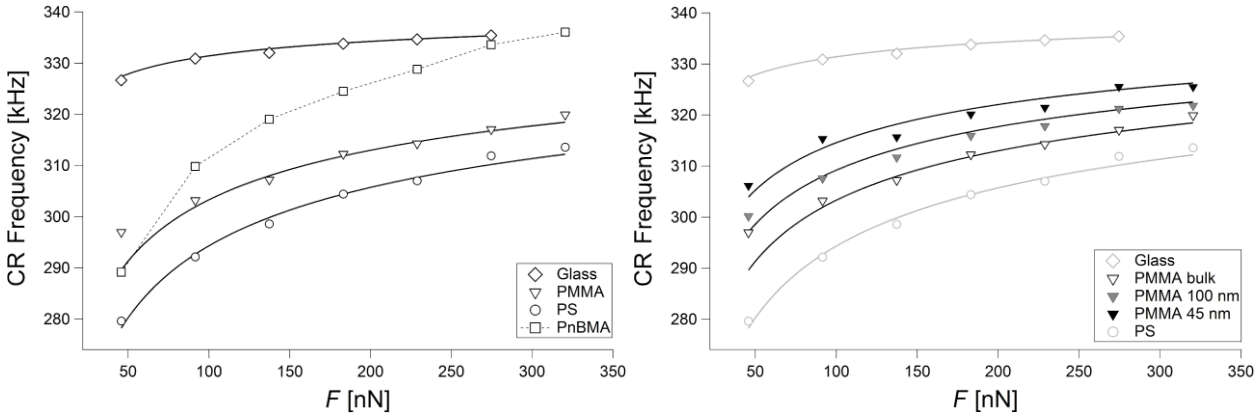

Figure 22 (Left) CR frequencies as a function of the force F on glass (diamonds), bulk PMMA (triangles), and bulk PS (circles), fitted with Equation 1 (black curves). CR frequencies on PnBMA (squares) are shown, too. (Right) CR frequency as a function of the force F on glass (diamonds), bulk PMMA (white triangles), bulk PS (circles, same curves as in the left panels), and on two PMMA films, 45 nm and 100 nm thick, (grey and black triangles, respectively). Curves are fitted with Eq. 3.1 (light grey and black curves). Adapted from Ref. [1.1].

The curves can be fitted quite exactly with Eq. 3.1, most of all those on glass and PS. Fitting parameters are the elastic modulus and the parameter γ. The three values of the elastic moduli obtained for glass, PMMA, and PS are 57 GPa, 6.2 GPa and 5 GPa, respectively, in agreement with previous measurements. The measured values of the elastic moduli of PMMA and PS are higher than the literature values for the respective bulk polymers. These higher values are due to inner stresses and the stretching of the polymer chains during spin coating. Furthermore, since CR measurements are performed at high frequencies, the time–temperature superposition principle leads to a stiffening of the sample.

The second fitting parameter, γ, is different for the three curves (0.982 for glass and 0.973 for PS and PMMA), although they have been acquired with the same cantilever. This contradicts the interpretation of γ as determined only by the relative position of the tip. Differences in the values of γ yielded by different measurements with the same cantilever indicate that commonly employed models are not appropriate for polymer samples. Not only anisotropies in the cantilever structure, tip mass, and lateral forces, but also plastic deformations, viscoelastic behavior, adhesion, and damping should be accounted for in models of the system. This would drastically increase the number of parameters needed for the description of the cantilever–sample system.

Also, CR frequencies acquired on bulk PnBMA are shown. The curve cannot be fitted with Eq. 3.1. This is due to the low elastic modulus and the higher chain mobility of PnBMA. As a consequence, PnBMA is very compliant and can be deformed plastically even with small loads. Hence, at high loads, PnBMA has been displaced laterally, i.e., the tip has carved a hole in the polymer film and is in contact with a very thin PnBMA film or even with the glass substrate. Therefore, the CR frequency goes from typical “polymer values” around 290 kHz at 50 nN to typical “glass values” around 330 kHz at 300 nN.

Turning to the measurements on two PMMA films with thickness values of 45 ± 5 nm and 100 ± 2 nm (right panel of Fig. 2), also fitted with Eq. 3.1, it is evident that the CR frequencies depend on the thickness. Hence, CR measurements enable to distinguish films of different thickness with moduli differing by 1–2 GPa. However, the thickness resolution is clearly worse than that of force–distance curves. A comparison with [3.3] shows that

force–distance curves enable the clear distinction of six different thickness values between a 45 nm thick film and bulk PMMA, whereas data scattering and the small differences between the frequencies (≅4 kHz) would hardly allow one to discern a further curve in the right graph of Fig. 2 between those corresponding to the 45 nm film and the 100 nm film or even between those of the 100 nm film and of the bulk sample.

A Good Practice Guide on the determination of polymer film thickness through force-distance-curves and CR methods has been produced.

A comparative analysis of the errors of the values of the moduli engendered by an uncertainty in the measured frequency (CR modes) or in the measured deflection (force–distance curves) shows that CR methods are more suitable than force–distance curves for the measurement of moduli larger than ca. 20 GPa. Bulk polymer samples and thin polymer films commonly have lower elastic moduli.

Force-distance curves

Measurements with the piezoresistive microprobes mounted in the Cypher AFM at BAM can be performed by exploiting either the laser signal via the common optical lever method or the output signal of the piezoresistive microprobe. Yet, these two signals cannot be acquired simultaneously.

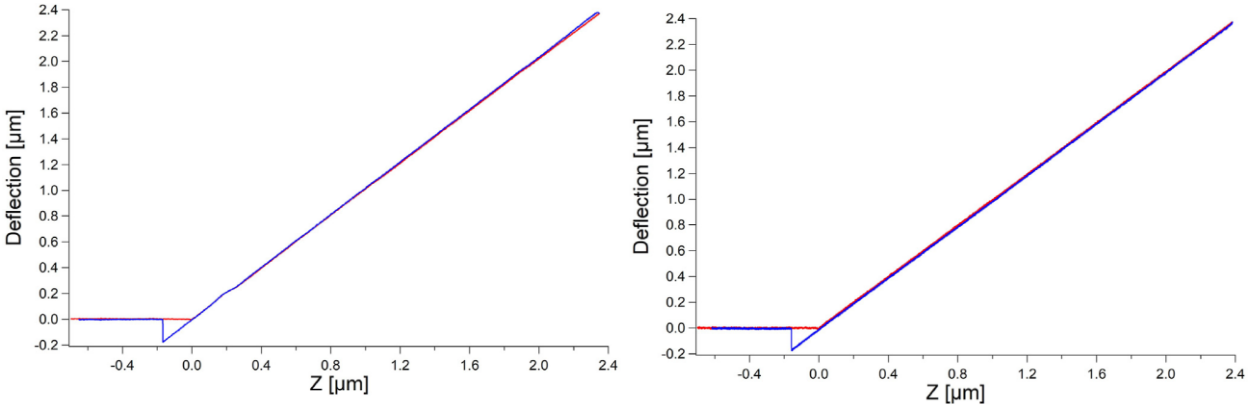

Figure 23 (Left) Deflection-displacement curve on a glass surface acquired in air with the optical-lever method at a frequency of 0.15 Hz. (Right) Same as in the top panel but using the piezoresistive output signal of the microprobe. The approach curves are in red, the retraction curves in blue. Adapted from Ref. [3.2].

Figure 23 shows deflection-displacement curves on a glass sample acquired with the optical lever method (left) and with the piezoresistive signal (right). The piezoresistive curve shows a considerably higher noise. For determining the noise of the microprobe and thereby the minimum detectable tip deflection, deflection-displacement curves were acquired on glass with different velocities and with different dwell times between approach and retraction. Figure 24 shows a curve with a dwell time of 600 s and ca. 20 s loading/unloading times. The red and black curves were acquired using the laser and the piezoresistive signals, respectively. The two insets show the 20 times magnified signals along the zero lines (bottom left) and during a part of the dwell time (top right).

For the noise analysis, three regions of the curves should be distinguished: the zero line (no contact between tip and sample), the dwell region (contact between tip and sample), and the contact line (contact between tip and sample during piezo extension). Four deflection-displacement curves with different load-dwellunload

In all three regions, the noise in the curves acquired with the piezoresistive signal is higher (typically twice as high, up to a factor of 2.9) than in the curves acquired with the laser signal. Since the microprobe used for the measurements is exactly the same, the differences between the noise measured with the piezoresistive signal and the laser signal cannot be due to the mechanical-thermal noise of the cantilever or to vibrations of the sample. They are caused by differences in the sensitivity of the two signals and the electronic noise caused by the piezoresistive Wheatstone bridge, the instrumentation preamplifier, and fluctuations of the bridge supply voltage.

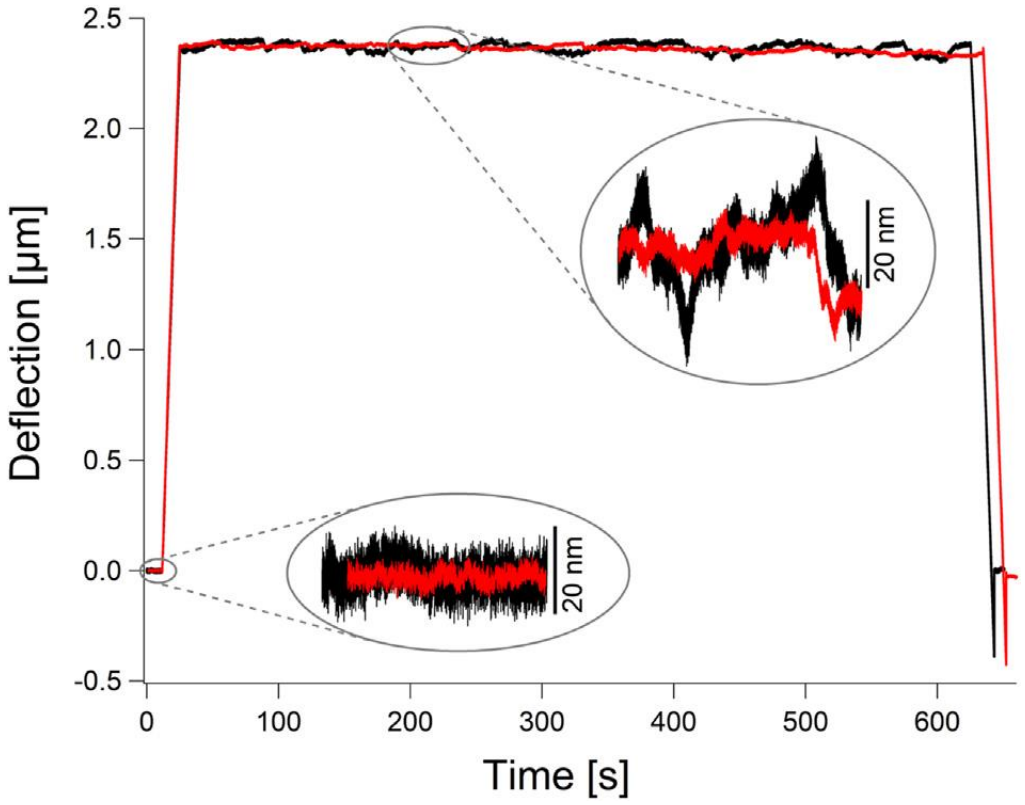

Figure 24 Deflection curves versus time on a glass surface with a dwell time of ca. 600 s and loading/unloading times of ca. 20 s. The red curve was acquired with the optical lever method, the black one with the piezoresistive signal. The insets show 20 times magnified signals along the zero lines (bottom left) and during a part of the dwell time (top middle). Reproduced from Ref. [3.2].

The comparison with a commercial AFM cantilever (PPP-NCSTAuD from Nanosensors, 152 µm long, 29 µm wide, 2.7 µm thick, elastic constant 7.3 N/m) shows that the noise of the microprobe, even with the laser signal, is 1 to 2 orders of magnitude higher.

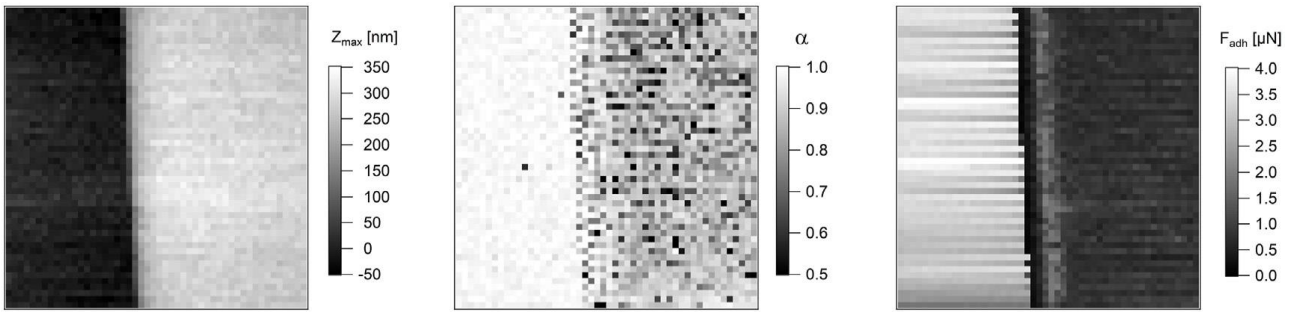

Figure 25 Force-volume at the border of an AZ 5214E film on silicon, acquired by exploiting the piezoresistive signal. Topography (left) and maps of the stiffness (middle) and of the adhesion force (right) are shown. The area of the maps is (25 µm)^2. The silicon substrate is on the left side of the maps, the polymer film on the right side. (Adapted from Ref. 2.

Figure 25 shows the results of a force-volume measurement on the edge of an AZ 5214E photoresist film on silicon, acquired by exploiting the piezoresistive signal. A force-volume is an array of force-distance curves (50 × 50 in this case) acquired on a certain area (25×25 µm^2) with the same maximum force (10 µN) and the same curve acquisition frequency (1 Hz). Three maps obtained from the force-volume measurement are shown: the topography (left), the stiffness (middle), and the adhesion force (right). The silicon substrate is on the left side of the maps, the polymer film on the right side. The lower stiffness and the lower adhesion force on the polymer film are as expected and in agreement with measurements performed with common cantilevers.

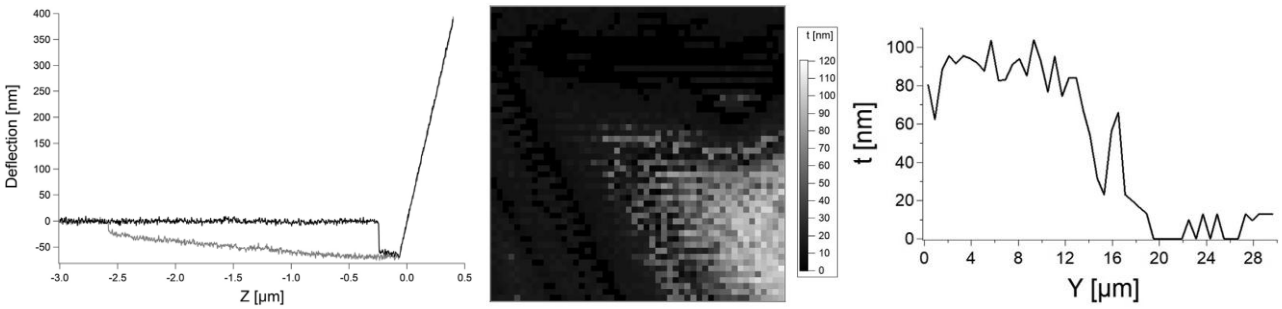

Figure 26 (Left) Deflection-displacement curve on a Lupranol film on glass surface acquired with the piezoresistive signal of the microprobe at 1 Hz. The approach curve is in black, the retraction curve in gray. (Middle) Map of the thickness of a Lupranol liquid film partially covering a glass surface, with 50×50 deflection-displacement curves over an area of (30 µm)^2. (Right) Vertical line profile across the thickness map at the horizontal position x = 27:8 µm. The origin of the coordinate system is in the lower left corner of the thickness map. Adapted from Ref. [3.2].

A further application of a force volume is the characterization of a thin liquid lubricant film on a substrate, for example Lupranol VP 9209 (BASF, Germany), a polyalkylene glycol, on a glass surface. A deflection-displacement curve is plotted in the left panel of Figure 26, with the approach part in black and the retraction part in gray. At a distance of 174 nm from the glass substrate, the tip jumps into contact with the liquid. Afterwards, the tip goes through the liquid film, which wets the tip, leading to a slightly attractive force, till the tip comes into contact with the glass substrate and the force becomes repulsive. In the retraction curve, the detachment from the liquid takes place at a distance of 2516 nm, which is much larger than the thickness of the Lupranol layer. For this lubricant, this is due to the formation of a meniscus and to the (partial) pinning of the three-phase contact line. Hence, the meniscus is stretched before the liquid detaches from the tip.

Such curves can be used to detect the thickness *t* of a liquid film. It is given as the distance between the jump-to-contact with the liquid and the jump-to-contact with the substrate, minus the deflection of the cantilever at the jump-to contact with the substrate. The thickness can be mapped, as shown in the middle panel of Figure 26. The map shows a liquid film with an average thickness of 90 nm in the bottom right corner of the scanned surface. As can be seen in the line profile in the right panel, although the distance between two successive curves (600 nm) is smaller than the width of the apex of the truncated tip, the borders of the liquid film can be detected quite well.

Additional curves have been acquired with shorter microprobes on several liquid lubricants.

A Good Practice Guide on the determination of the thickness of liquid films by means of force-distance curves has been produced.

Conclusion

To summarise, BAM assisted by TUBS successfully achieved the objective. Mains results are:

- CR methods are more suitable than force–distance curves for the measurement of moduli larger than ca. 20 GPa and not for polymers
- Despite the quite high noise, force-distance curves acquired with microprobes can be used to characterize quantitively the stiffness and adhesion of polymer films and the thickness of liquid films.

[3.1] S. Friedrich, B. Cappella. Beilstein J. Nanotechnol. 2020, 11, 1714–1727.

[3.2] M. Fahrbach, S. Friedrich, H. Behle, M. Xu, B. Cappella, U. Brand, E. Peiner. Measurement: Sensors 15 (2021) 100042

[3.3] D. Silbernagl, B. Cappella. Surf. Sci. 2009, 603, 2363–2369.

Objective 4: *To develop the integration of microprobes into manufacturing machines, roll grinding machines and wear measuring machines and to develop measuring methods resistant against ambient influences.*

Integration of a microprobe into a manufacturing machine

Bmt developed a piezoresistive MicroProfiler with 5 mm long microprobes and an integrated feed unit aiming at scanning speeds up to 15 mm/s. First results were obtained with a prototype system which allowed measurement speeds up to 8 mm/s. A new amplifier electronic was developed in order to reduce noise during measurements. Due to Corona-virus restrictions the electronic could not be completed within the project

duration. To integrate the MicroProfiler into a microfinishing machine TT developed a machine-probe interface. Measurements with a MiniProfiler from BMT were made to evaluate the performance of the developed adapter and to measure the vibration amplitudes and frequencies of the microfinishing machine.

Development of a microprobe unit with integrated feed-unit for scanning speeds up to 8 mm/s

The performance of the developed MicroProfiler prototype was measured using a sinusoidal roughness standard (with a maximum height of RzDIN = 3.04 µm and a wavelength of 100 µm) and a flat glass plate. Scanning speeds of the integrated feed-unit from 0.5 mm/s up to 8 mm/s were successfully tested. Higher scanning speeds are not possible because the acceleration of the scanning table used is limited and not sufficient to obtain higher scanning speeds.

Test measurements on a sinusoidal roughness standard

Nine scanning speeds from 0.5 mm/s up to 8 mm/s were tested and for each 25 measurements were made. For all profiles the noise, the maximum height RzDIN and the available measurement length were calculated in order to determine the maximum scanning speed. The measurement and evaluation conditions were a cut-off wavelength of 0.8 mm, 3000 measurement points and a measurement length of 6.0 mm. The measured profiles were aligned using a linear regression. It was found that the measurement noise does not increase significantly with increasing measurement speed from 0.5 mm/s up to 8 mm/s, so that this criterion was not taken into account to determine the maximum scanning speed.

During measurements with a scanning speed of v = 7 mm/s a saturation of the amplifier of the MicroProfiler at a z-value of 117 µm was observed. This is a problem of the MicroProfiler signal electronics and will be solved with the new electronic version under preparation.

At the highest possible speed of v = 8 mm/s another problem arises. The measurable length is limited to approximately 3.3 mm instead of 6 mm due to the longer acceleration times at higher speeds. The scanning distance of the integrated feed unit is divided into three areas: acceleration part, measurement part and braking part. Even at higher speeds, the braking distance is very short and therefore negligible, but the increasing acceleration part decreases the usable measuring length. This problem cannot be solved easily, and a reconstruction of the traverse unit would be necessary.

Thus, from these observations it can be concluded that maximum scanning speeds of up to 8 mm/s are in principle possible, but a reduced measurement length has to be taken into account for the highest currently possible scanning speed of 8 mm/s.

A further evaluation of the RzDIN values of the measured profiles was done showing quite comparable RzDIN values up to v = 8 mm/s. Only for v = 7 mm/s a deviation of 5 % due to the saturation of the MicroProfiler amplifier was observed. Thus, also the roughness evaluation confirms that scanning speeds up to 8 mm/s are possible with the MicroProfiler prototype.

Test measurements on a flat glass plate

Test measurements at scanning speeds up to 8 mm/s were also made on a flat glass specimen. It could be seen that the signal noise increases with scanning speed by a factor of eight from 5 nm at 0.5 mm/s to 43 nm at 8 mm/s. These results confirm previous measurements results [1] where a comparable increase in noise was observed.

Adaptation of a miniprofiler into a microfinishing machine

The aim was the integration of a roughness-measuring system into a microfinishing machine. In contrast to a measuring laboratory, the environment of a production machine is characterized by several interfering influences like the appearance of vibrations and fluids. Within the project it should be evaluated how reliable in-process roughness measurements can be done in such an environment.

For the integration of the measuring system, *Thielenhaus Technologies* choosed a roundtable machine from type *MicroStar 286*. The machine can be equipped with up to seven stations to machine the workpieces. Instead of using a finishing unit to machine the workpiece, the station can also be used for a measuring unit like the *MiniProfiler* from *Breitmeier Messtechnik*. In order to integrate the M*iniProfiler* into the microfinishing machine *Thielenhaus Technologies* developed a machine-probe interface as shown in figure 1. The adapter can lift and sink the measuring unit. Additionally, the mechanical adapter provides an interface for compressed air in order to protect the M*iniProfiler* from lubricants.

The roughness measurements were conducted on typical microfinish applications like gear wheels and sealing surfaces. Usually, the machined surfaces are characterized by a smooth surface with low surface roughness.

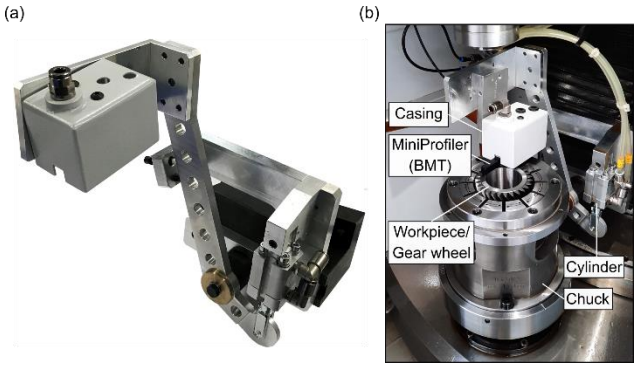

Figure 27: (a) Mechanical adapter for the Miniprofiler, (b) Assembled and integrated adapter

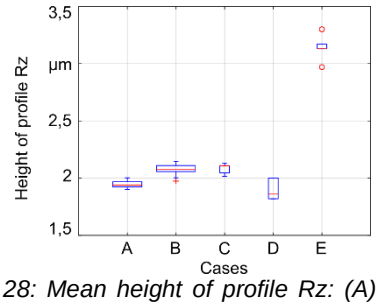

Figure 28: Mean height of profile Rz: (A) without external influences, (B) rotating spindles, (C) oil on the workpiece surface, (D) compressed air with a pressure of p = 0.5 bar, (E) compressed air with a pressure of p = 1 bar

In-process roughness measurement on a microfinishing machine

To get a comprehensive understanding of the technical possibilities doing an in-process roughness measurement with the *MiniProfiler,* five different cases were analyzed. As shown in *Figure 28*, the reliability of the roughness measurement without any external influences is good. Within 20 measurements (measurement length L = 5.6 mm, λc = 0.8 mm) the mean height of profile Rz according to ISO 21920-2 varies between Rz = 1.9 - 2.0 µm. The infeed speed during the measurements was varied between v_f = 0.5 mm/s and v_f = 2 mm/s in order to prove the reproducibility of the results. Within this range of infeed velocity, there are no significant deviations. In case of doing the measurements with rotating spindles or with oil on the workpiece surface, the height of profile Rz increased to Rz = 2.1 µm. The range of the measured values increased as well to ΔRz = 0.2 µm. Even though the range of the measured values is twice as high compared to the measured values without any external influences, an in-process measurement is imaginable with some restrictions concerning the reliability.

In contrast to these promising results, the roughness measurements with compressed air showed a different behavior. Using compressed air with a pressure of 0.5 bar resulted in a height of profile between Rz = 1.8 µm and Rz = 2.0 µm. Increasing the pressure in order to realize a better protection of the *MiniProfiler* worsened the results dramatically. With an air pressure of 1 bar the height of profile increased to Rz = 3.1 µm with a range of ΔRz = 0.3 µm.

Vibration measurement on a microfinishing machine

Even if the vibrations showed a minor influence on the resulting roughness value, a further detailed analysis was realized in order to detect the reason for the deviation. Several measurements were carried out with a speed variation of two workpiece spindles denoted s2 and s4 on the stations next to the measurement station. In contrast to a normal roughness measurement, these measurements were done without any infeed of the MiniProfiler. With this strategy, it was possible to visualize the deviations resulting from the vibrations. Depending on the speed of the workpiece spindles, a periodic signal with a specific frequency was detectable. *Thielenhaus Technologies* provided the measurements for *PTB* for further Fourier analysis. In the obtained spectra distinct oscillation frequencies can be observed. From the Power Spectral Density (PSD) investigation it can be concluded that observed main vibration frequencies are 13 Hz and higher harmonics for one spindle (s4) and 26 Hz and higher harmonics for the second spindle (s2). These values compare very well with the frequency of the rotation spindle of 800 rotations per minute which corresponds to 13.3 Hz. The vibration amplitudes reach up to 300 nm for spindle s4 and up to 120 nm for spindle s2. The amplitude values are confirmed by Root Mean Square (RMS) roughness values calculated for all profiles. Noise levels go up to RMS = 564 nm for spindle s4 at 800 rotations/minute and 127 nm for spindle s2.

The measured vibration frequencies are not much affected by the damping of the MiniProfiler and thus show us, that vibration frequencies up to 1 kHz occur.

Integration of microprobes into roll grinding machines

VTT with support from TUBS designed and manufactured the electronics for a microprobe and performed tests in laboratory. RRI with support from VTT designed and manufactured the mechatronics for a microprobe to be attached to grinding machine.

Tests were carried out in the actual grinding machine in an industrial environment. The results from the tests were very promising, and the industrial measurements show good correlation with the lab results. The

performed tests showed acceptable measurement errors for selected parameters. Although not perfect these initial results are acceptable and promising. The development of the commercial version is and will be continued. Also, RRI has received a request for quotation from one potential customer.

Tests performed in the laboratory and in an industrial setting showed measurement deviations of less than 6% and less than 3%, respectively, for selected parameters (Ra, Rz and Rsm). These values are good compared to other instruments affordable to industry.

Description of the microprobe configuration

In this study, a preamplifier electronics printed circuit board (PCB) design from Technische Universität Braunschweig [4.10] was redesigned for this purpose. It includes a low noise voltage regulator for the Wheatstone bridge supply and an instrumentation amplifier for the bridge output voltage. The dimensions of the PCB were adjusted to a width of 50 mm and a length of 25 mm, which is better suited to the equipment intended for the industrial measurements. The bridge voltage was increased from 1 V to 3 V. The amplification gain was decreased to 61 to compensate for the voltage increase, reducing the noise amplification.

Frequency properties of the selected microprobe have been studied in earlier research [4.10] and the resonant frequency is calculated to be 2.8 kHz. Contact resonant frequency is much higher and slightly dependent on sample material, 9.6 to 16 kHz and 14.1 to 14.3 kHz. Using measurement speeds up to 10 mm/s wavelengths down to 1 µm can be detected.

Microprobe sensor set-up for roll measurements

Due to fragility of the microprobes, a sliding skid was developed and used in the tests to protect the microprobe from too high deflections. The skid also works as a reference or datum for the measured profile. The roll is cylindrical, and the skid has the shape of a plane giving a cylinder/plane contact. The sliding skid is sufficient for measuring roughness and acceptable for measuring waviness to within a few millimetres. The integration of the microprobe into the roll measuring device is described in detail in the thesis [4.11].

A microprobe holder was designed specifically for this study to enable mechanical installation of the microprobe on a roll measuring device. The microprobe is mounted on one of the measuring probes of the existing roll geometry device. This allows the diameter variation or alignment errors of the roll to be ignored during roughness measurements, as the measuring probe moves radially relative to the roll. Also, the motion axes of the grinding machine can be used to perform roughness measurements. The microprobe was placed in contact with the roll on an axis moving radially relative to the roll. Measurements were performed on an axis moving parallel to the longitudinal axis of the roll. The measuring process was carried out in the same sequence each time: first make contact, then start the movement along the longitudinal axis of the roll.

Figure 29 shows the mounted microprobe and holder design on the left and an exploded view of the holder assembly on the right. The assembly consists of five individual parts and a nut, which belongs to the original S4 design. When the microprobe is mounted, there is a 12-degree angle between the roll surface and the microprobe.

With the microprobe integration used in this study, the diameter range of the rolls that can be measured is from 300 mm to 2000 mm. Measuring length is not limited by the integration method. However, the tip durability of the microprobe is limited, and the size of the grinding machine determines the longitudinal travel along the roll.

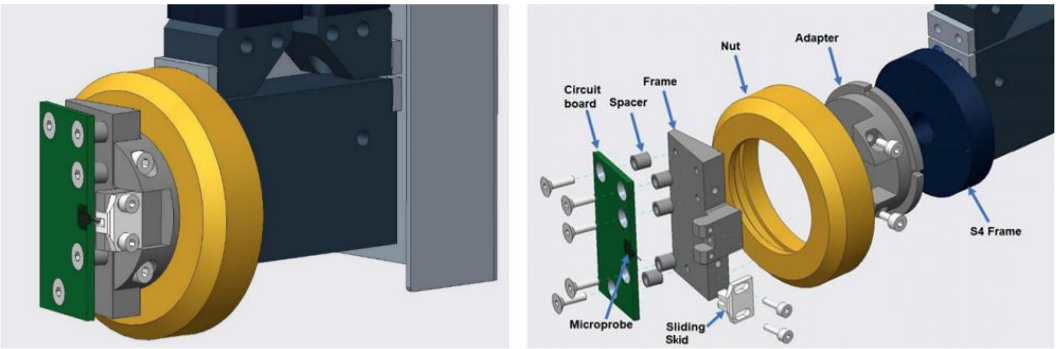

Figure 29 CAD design (left) and exploded view (right) of microprobe integration in a roll measuring instrument.

Measurements

Rolls used in paper machines are large and roughness measurements are meaningful with sample spacing of about one micron or less. Therefore, it would not be economical to measure a roughness profile consisting of

10^6 points and length 10 m. Although this would be possible and, in some cases, meaningful here profiles of 100 mm length were measured. With this length the overlapping of grinding can be detected. From these profiles' roughness parameters Ra, Rz and Rsm defined in ISO 4287 were calculated.

To inspect the complete roughness geometry map of the roll it is suggested to measure 100 mm long profiles at 1000 mm intervals in the axial direction of the roll. To get the complete roughness map of the roll the roll should be rotated by for example one degree and the profile measurements would be repeated. However, if the results of roundness measurements are satisfactory, angular step of 90 degrees are recommended.

As the microprobe is equipped with a sliding skid, it has limitations regarding measurements of waviness. However, for the purpose of feedback for the grinding process it might be useful to perform a waviness analysis. Short wavelengths are filtered out using a cut-off wavelength of 0.8 mm. This cut-off wavelength is small compared to the dimensions of the sliding skid. Now three large, repeated valleys are visible in the profiles, which tell us that there is a small mismatch between the dimensions of the grinding wheel and the pitch control of its movement. This is an additional example of useful data provided by microprobe measurements.

[4.10] M. Fahrbach *et al.*, "Customized piezoresistive microprobes for combined imaging of topography and mechanical properties," *Measurement: Sensors*, vol. 15, no. September 2020, p. 100042, 2021, doi: 10.1016/j.measen.2021.100042.

[4.11] T. Lindstedt, "Mechanical integration of microprobe as surface roughness tester on roll measuring device," 2020.

Integration of microprobes into wear measuring machines

The introduction of fast microprobes into tribological testing systems has been demonstrated through their introduction into four different test systems. These were a scratch testing system, a pin-on disc test system, a reciprocating tribometer and a microtribometer that could either be used ex situ on the laboratory bench, or in situ inside an SEM. It was found that excellent results were obtained from the in-situ measurements giving high resolution profiles of the wear damage that had been developed during tribological tests. The quality of the measurements and their sensitivity was good and compared well quantitatively with conventional post-test measurements.

Most of the tests that were carried out in an interrupted testing mode where the test was run for a period, sample movement stopped, a profile measurement made and then the cycle repeated until the end of the test. However, one test was also successfully carried out where the test sample was moving throughout the test and it was found that good measurements of wear damage were also obtained in this case.

The utility of the fast microprobes is illustrated by results from two test systems. Firstly, *Fig. 30* shows quantitative results from the microprobe profile measurements in a scratch test experiment where a diamond stylus formed scratches across an alumina sample. *Fig. 30*a shows the raw profiles taken across the scratch. It should be noted that the surface of the alumina test sample was quite rough, as shown by the profile over the surface away from the scratch itself. The profiles were registered with one another by correlating the profiles in these regions away from the scratch. The progressive increase in the depth of the scratch can be seen clearly.

Then the zero repeat scratch profile (the profile of the surface before any scratches) was used as a reference profile and was subtracted from the other profiles. There is some remnant variation in the profiles outside the scratched area due to the uncertainty in the position of the microprobe scan from one profile to another. The profiles across the scratch were also zeroed by setting the average height of the profile away from the scratch to zero.

The area of the scratch can be found by integrating the area of the profiles. *Fig. 30*b shows how the calculated area of the scratch increases with the number of scratch repeats. This provides good quantitative information on the degree of damage and its relationship to the number of scratches. This compares with the conventional method of monitoring how the damage increases with the number of scratch repeats which is to carry out a sequence of different scratches at different repeats which are individually measured after the scratching to determine the area of the scratch for a given number of repeats.

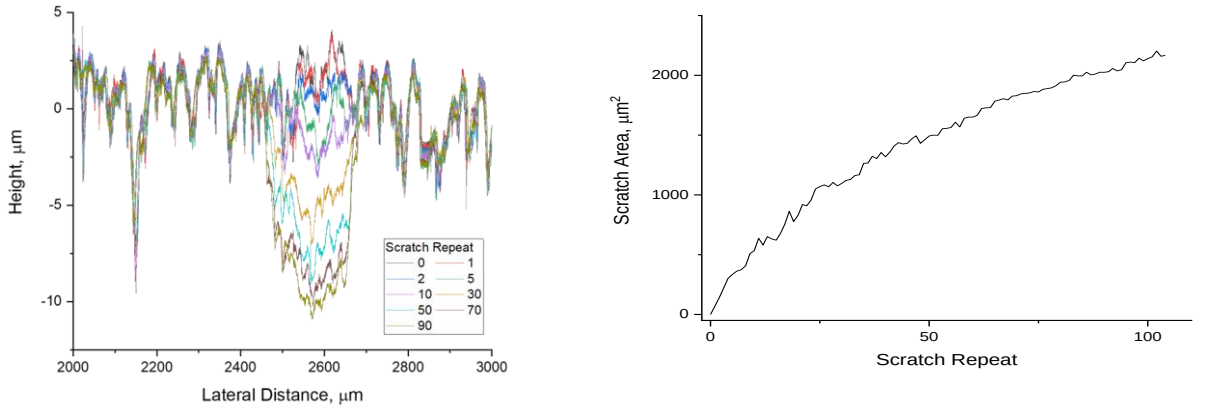

Fig. 30. Results from measurements with scratch testing system, a) (left) raw profiles taken across scratch at different number of scratch repeats, c) variation of calculated scratch area with scratch repeat.

A schematic of the pin-on disc tribometer that was used to explore the utility of the TUBS / PTB microprobe for in situ measurement is shown in Figure 8. The system is fitted with an optical linescan camera which can be used to image the wear track in situ and in real time as it is formed, together with a multipoint chromatic aberration probe that forms in situ real-time non-contact profiles across the wear track [4.21]. The TUBS/PTB microprobe was mounted on the test system and orientated so that profiliometric scans could be made perpendicular to the wear track. The main experiment that was carried out was a rotating scratch test where a Rockwell 200 µm radius diamond indenter was pushed into a rotating disc of steel [4.22].

Figure 9 shows the quantitative results from the experiment. Figure 9a shows a waterfall plot of the measurements with the microprobe which clearly show how the depth and width of the groove develops with increasing number of sample rotations. These results are compared with the simultaneous output from the multipoint chromatic aberration probe in Figure 9b. The overall form of the groove is similar, but there is less detail in the chromatic probe output. This is also shown in Figure 9c which shows a direct comparison of the profiles for three rotations of the disc. Again, the form of the profiles is very similar with much more detail in the profiles from the microprobe. This is due to the increased lateral resolution of the microprobe compared to the chromatic aberration probe which is physically limited to 180 measurement points. By integrating the profiles, the area of pile up (material raised above the level of the surface outside the scratch), area of the groove (cross-section of area below surface), and area of material lost from surface (groove area – pile-up area). It can be seen that the results obtained from both systems are very similar.

In summary the introduction of fast microprobes into wear testing systems proved to be relatively simple as long as reasonable care was taken to integrate the measurements obtained from the microprobes into test systems. The quality of the quantitative information that is provided together with the opportunity to acquire real time in situ results during tests make the use of fast microprobes a useful tool that should be introduced more widely into wear measuring systems.

One drawback of the microprobes is that they are very fragile, so great care is needed to ensure that they are handled carefully. To help to protect the microprobes a simple overload protector was designed and fabricated using polymeric additive manufacturing. This overload protector was practically tested when a sample slipped in a tribological test bringing the microprobe head down sharply onto the opposing sample. The overload protector did its job preventing damage to the microprobe.

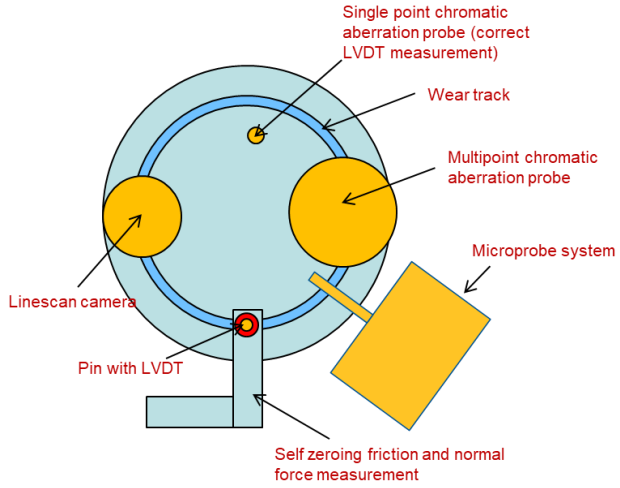

Fig. 31. Schematic of NPL integrated pin on disc tribometer

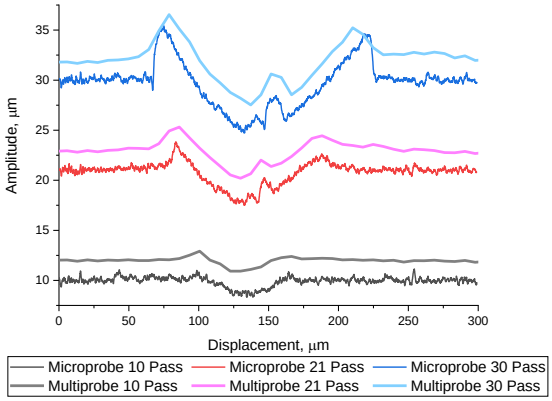

Fig. 32. Results from rotating scratch test on steel sample, details of comparison between profiles for 3 different number of rotations, for the two different microprobes.

[4.21] STIL Chromaline line sensor
[4.22] M Gee, T Kamps, P Woolliams, J Nunn, K Mingard, In Situ Real Time Observation of Tribological Behaviour of Coatings, accepted for publication in Surfaces and Coatings

Conclusion

To summarize, the project almost completely achieved the objective by the development and testing of the integration of microprobes into manufacturing machines, roll grinding machines and wear measuring machines. In detail:

- at Thielenhaus Technologies, a large supplier of microfinishing machines, a conventional MiniProfiler from Breitmeier Messtechnik was firstly tested on a microfinishing machine. These tests showed acceptably reliability even with oil on the workpiece. Microprobes with integrated feed-unit for measurement speeds up to 8 mm/s were developed and successfully tested by Breitmeier. Further tests with these microprobes on microfinishing machines need to be done in future.
- Rollresearch with support from VTT and TUBS designed and manufactured the mechatronics for a microprobe to be attached to a grinding machine. Tests performed with a grinding machine in a paper plant showed promising results and commercialization of the mechatronics including a microprobe is planned.
- at NPL a microprobe was integrated into a wear measuring machine, and it was concluded to be a useful tool in the future.
- one drawback with microprobes experienced in all tested applications is that they are fragile and need protection for overload.

5 Impact

The consortium organised two stakeholder meetings/workshops. The first took place at the Euspen international conference on June 3, 2019 in Bilbao. Among the 23 participants, nine were from industry (Bruker, Micro Epsilon, Sub Micron Tooling BV, Bestec GmbH, Carl Zeiss SMT GmbH, Zygo Corproration, Egile mechanics) and fourteen from universities and research institutes from ten different countries all over the world (USA, China, Japan, United Kingdom, Spain, Netherlands, France, Italy, Czech Republic and Germany). The project was well received and the stakeholders' provided suggestions on how to more closely align the work of the project to their needs.

The second meeting was on-line and held on June 23, 2021 for the presentation of project results to 20 stakeholders drawn from the same audience as the previous meeting. At this meeting there was a lively discussion of topics relating to tip wear of fast silicon tips, improving CR metrology using spherical diamond tips, measurement errors due to cantilever oscillation and increasing damping.

In addition, the consortium has held discussions with industry to find out the metrological requirements of end-

users. One request from audio industry focusses on the measurement of the complex modulus of elasticity for polymer materials for frequencies up to 20 kHz. This modulus is necessary for the modelling and simulation of the dynamic behaviour of devices. A follow up project is planned to address this issue.

A further request came from an instrument manufacturer who looked for traceability of his AFM based indentation modulus measurement device for applications in breast cancer detection. Again a follow up project is planned to address this request.

The project has held five training courses for the consortium on i) how to use the microprobes without feed-units for topography and CR measurements, ii) on the determination of 2d tip form on the machine, iii) on how to determine noise and drift of microprobes, iv) on the improvement of the project and v) on measuring mechanical properties of polymers with AFM. These courses have enabled industrial project partners to develop new microprobe adapters and to apply microprobe for topography and mechanical property measurements, to exactly determine the 2d tip radius, to determine the metrological properties of microprobes and for the first time to apply long microprobes on a commercially available AFM and compare the microprobe performance with that of one of the best AFM instruments available on the market [10]. Two master theses have been published and nineteen presentations have been made at conferences.

Impact on industrial and other user communities

This project worked to support industrial users of tactile surface texture metrology by developing new fast tactile microprobes for integration into their manufacturing machines however there remained a significant challenge to convince stakeholders of this new technology. The project vigorously promoted the benefits of piezoresistive microprobes that create a faster and cheap tactile measurement system with two functionalities: topography and mechanical surface parameters to end users in high precision mechanical engineering used in transportation, power generation, paper production and the mining industries. Specific examples include:

- *The development of new microprobe devices and prototypes for simultaneous roughness and modulus mapping measurements on-the-machine.* New microprobes with integrated electrothermal actuator, diamond tips, different microprobe holders and complete microprofilers with integrated feed-unit developed in this project allow industry to integrate the microprobes onto micro-finishing machines, high-tech roll measuring and control systems, tribometers and dimensional surface measuring machines. GETec Microscopy GmbH and nano analytic GmbH [11] have built small adapter boards with which the microprobes can be used on their fast-measuring machines. This will allow industries developing structures, where only the long slender microprobes can enter in, to measure topography and mechanical parameters of their products. The PCBs developed in this project can be used by researchers to measure topography and mechanical parameters on manufacturing machines. New plastic transport boxes have been developed which allow the safe transport of the sensors and even the sending of the probes by mail. All these devices are available on request.
- *A new method for the tip form measurement on-the-machine.* A new method to measure the 2d tip form of microprobe tips has been successfully tested and a Good Practice Guide was developed. The Good Practice Guide describes the project's newly developed calibration methods, conditions under which they are to be operated, procedures to be followed, target uncertainties and the best working practices.
- *A new method for the determination of the maximum scanning speed at a given probing force.* A Good Practice Guide on the setting of probing force dependent on the hardness of the material to be measured and the maximum scanning speed to avoid tip-flight was developed. Developers of tactile surface profile and roughness measuring instruments, microfinish machine manufacturers, roll measuring machine manufacturers, tribology measurement instrument manufacturers and similar organisations will benefit from these results.
- *Two new measurement methods: CR and FDC.* Two companies showed interest in these new methods. One is interested in dynamic FDC measurements for the dynamic measurement of the elastic properties of polymer materials, which is needed for the optimization of materials in acoustic products. The second company is interested in the traceability of the measured tip form of AFM tips and probing forces which are used for the early detection of cancer using AFM stiffness measurements.
- *The development of new reference materials and calibration standards.* Beneficiaries will be organisations interested in modulus mapping and those providing the microprobing systems. In the long-term TUBS and PTB can supply the calibration and reference standards.

Impact on the metrology and scientific communities

The project benefited from a variety of partners, such as NMIs, academic organisations, and industry as well as collaborators from microfinishing, rolls and tribology. The project has facilitated joint working between companies, NMIs and the scientific community in developing microprobe PCBs for different applications. The

project has also facilitated the training of the next generation of metrologists through the five training courses mentioned above. The project has had direct impact on the scientific community through the significant use of project's outputs by the scientific research community as indicated by the high number of scientific publications.

Impact on relevant standards

The project concentrated on the standardisation of the metrology for piezoresistive long microprobes, i.e. (i) tip form measurements on-the-machine, (ii) permitted probing forces in dependence of material elasticity, hardness and scanning speed, (iii) elastic modulus measurement using CR and (vi) thickness of lubricant films using FDC.

First steps have been made to standardize the measurement of probing forces and the estimation of plastic deformation during tactile measurements. Interactions with the German DIN standardization committee NAFuO 027, the technical committee 03-03 on the influence of probing force and scanning speed on plastic deformation of soft layers on hard substrates led to the presentation to ISO TC 213 WG 16 of the fast piezoresistive microprobes culminating in a first draft of a new work item proposal in 2019. The committee received the draft with interest and started an intensive discussion about the transfer, e.g. into the surface roughness standard ISO 25178.

During the project, several new measurement methods based on the application of piezoresistive microprobes have been developed and these have been promoted to standardisation committees concentrating on areal surface metrology (ISO TC 213 WG 16 Areal and profile surface texture), on mechanical parameter measurements (ISO TC 164 Mechanical testing of metals), on wear measurements (ASTM G02 Wear and Erosion) and on ceramic coatings (ISO TC 206 WG10 Ceramic Coatings).

The project developed Good Practice Guide "Calibration of tip radius of fast microprobes on-the-machine" was presented by the partners to VDI/VDE GMA 3.41 subcommittee, as this organisation specialises in guideline development.

Longer-term economic, social and environmental impacts

The direct environmental impact of the project comes from the reduction in manufacturing waste on micro-finishing machines, which can be achieved through the new microprobes that this project will enable. The optimisation of product quality will lead to an increase in manufactured part quality and at the same time decrease associated costs. Reduction of waste in manufacturing has a direct economic benefit, as does a reduction in the amount of raw materials used, which can both be obtained by zero defect quality. The improved measurement capabilities and more rapid manufacturing developed by this project will support an improvement in industrial quality control and hence allow more rapid innovation, cheaper prototyping, and an overall reduction in time to market. Based on this, the machine tool industry (exports reached a record level of 19 billion euros in 2016), the printing machine industry, surface foil industry and the wear testing machine industry will be able to strengthen their position on the world market.

6 List of publications

1. Brand, U.; Xu, M.; Doering, L.; Langfahl-Klabes, J.; Behle, H.; Bütefisch, S.; Ahbe, T.; Peiner, E.; Völlmeke, S.; Frank, T.; et al. Long Slender Piezo-Resistive Silicon Microprobes for Fast Measurements of Roughness and Mechanical Properties inside Micro-Holes with Diameters below 100 µm. *Sensors* **2019**, *19*, 1410, https://doi.org/10.3390/s19061410.
2. Behle, H.; Brand, U. P2.7 Mode Analysis for Long, Undamped Cantilevers with Added Diamond Tips of Varying Length for Fast Roughness Measurements. *SMSI 2020 - Sens. Instrum.* **2020**, 238–239, https://doi.org/10.5162/SMSI2020/P2.7.
3. Fahrbach, M.; Peiner, E. P2.10 Entwicklung Eines Taktilen Mikrotaster-Messsystems Für Hochgeschwindigkeitsmessung von Form, Rauheit Und Mechanischen Eigenschaften. In Proceedings of the Proceedings; June 25, 2019; pp. 720–725, https://doi.org/10.5162/sensoren2019/P2.10.
4. Fahrbach, M.; Peiner, E. A6.3 Higher-Mode Contact Resonance Operation of a High-Aspect- Ratio Piezoresistive Cantilever Microprobe. *SMSI 2020 - Sens. Instrum.* **2020**, 89–90, https://doi.org/10.5162/SMSI2020/A6.3.
5. Fahrbach, M.; Krieg, L.; Voss, T.; Bertke, M.; Xu, J.; Peiner, E. Optimizing a Cantilever Measurement System towards High Speed, Nonreactive Contact-Resonance-Profilometry. *Proceedings* **2018**, *2*, 889, https://doi.org/10.3390/proceedings2130889.
6. Setiono, A., et al., In-Plane and Out-of-Plane MEMS Piezoresistive Cantilever Sensors for Nanoparticle Mass Detection, Sensors 2020, 20(3), 618; https://doi.org/10.3390/s20030618

7. Fahrbach, M.; Friedrich, S.; Cappella, B.; Peiner, E. Calibrating a High-Speed Contact-Resonance Profilometer. *J. Sens. Sens. Syst.* **2020**, *9*, 179–187, https://doi.org/10.5194/jsss-9-179-2020.
8. Setiono, A.; Fahrbach, M.; Deutschinger, A.; Fantner, E.J.; Schwalb, C.H.; Syamsu, I.; Wasisto, H.S.; Peiner, E. Performance of an Electrothermal MEMS Cantilever Resonator with Fano-Resonance Annoyance under Cigarette Smoke Exposure. *Sensors* **2021**, *21*, 4088, https://doi.org/10.3390/s21124088.
9. Fahrbach, M.; Peiner, E.; Xu, M.; Brand, U. A5.4 Self-Excited Contact Resonance Operation of a Tactile Piezoresistive Cantilever Microprobe with Diamond Tip. *SMSI 2021 - Sens. Instrum.* **2021**, 73–74, https://doi.org/10.5162/SMSI2021/A5.4.
10. Fahrbach, M.; Friedrich, S.; Behle, H.; Xu, M.; Cappella, B.; Brand, U.; Peiner, E. Customized Piezoresistive Microprobes for Combined Imaging of Topography and Mechanical Properties. *Meas. Sens.* **2021**, *15*, 100042, https://doi.org/10.1016/j.measen.2021.100042.
11. Reuter, C.; Holz, M.; Reum, A.; Fahrbach, M.; Peiner, E.; Brand, U.; Hofmann, M.; Rangelow, I. A6.2 Applications of Tactile Microprobes for Surface Metrology. *SMSI 2020 - Sens. Instrum.* **2020**, 87–88, https://doi.org/10.5162/SMSI2020/A6.2.
12. Teir, L.; Lindstedt, T.; Widmaier, T.; Hemming, B.; Brand, U.; Fahrbach, M.; Peiner, E.; Lassila, A. In-Line Measurement of the Surface Texture of Rolls Using Long Slender Piezoresistive Microprobes. *Sensors* **2021**, *21*, 5955, https://doi.org/10.3390/s21175955.
13. Xu, M.; Li, Z.; Fahrbach, M.; Peiner, E.; Brand, U. Investigating the Trackability of Silicon Microprobes in High-Speed Surface Measurements. *Sensors* **2021**, *21*, 1557, https://doi.org/10.3390/s21051557.
14. Friedrich, S.; Cappella, B. Application of Contact-Resonance AFM Methods to Polymer Samples. *Beilstein J. Nanotechnol.* **2020**, *11*, 1714–1727, https://doi.org/10.3762/bjnano.11.154.
15. Nyang'Au, et al., MEMS-Based Cantilever Sensor for Simultaneous Measurement of Mass and Magnetic Moment of Magnetic Particles, Chemosensors 2021, 9(8), 207; https://doi.org/10.3390/chemosensors9080207.
16. Lindstedt, T. Mechanical Integration of Microprobe as Surface Roughness Tester on Roll Measuring Device. Master Thesis Aalto Univ. Libr. **2020,** http://urn.fi/URN:NBN:fi:aalto-202003222560.
17. Teir, L. Microprobe Surface Roughness Characterization. *Master* Thesis Aalto Univ. Libr. **2020**, http://urn.fi/URN:NBN:fi:aalto-2020122056319.
18. Xu, M.; Zhou, Z., Ahbe, T.; Peiner, E.; Brand, U.; Using a Tip Characterizer to Investigate Microprobe Silicon Tip Geometry Variation in Roughness Measurements, *Sensors* **2022**, 22(3), 1298, https://doi.org/10.3390/s22031298.

This list is also available here: https://www.euramet.org/repository/research-publications-repository-link/

7 Contact details

Uwe Brand

PTB

Bundesallee 100, D-38116 Braunschweig, Germany

+49 531 592 5100

uwe.brand@ptb.de